

THE INSTITUTE OF PAPER CHEMISTRY

Appleton, Wisconsin

STUDY OF FIBER TUBE AND CORE PERFORMANCE

Project 2906

Report Two

A Progress Report

to the

FIBRE TUBE AND CORE RESEARCH GROUP

January 14, 1972

## TABLE OF CONTENTS

	Page
SUMMARY	1
INTRODUCTION	5
MATERIALS	7
Core Dimensions and Construction	7
Fabrication Procedures	8
CONDITIONING	14
TEST PROCEDURES	16
Core Tests	16
Core Stock and Liner Tests	18
DISCUSSION OF RESULTS	20
Properties of Core Stocks and Liners	20
Core Performance Results	24
Axial Crush	24
Effect of Diameter and Wall Thickness	24
Axial Strength Equation	33
Side Crush	37
Effect of Diameter and Wall Thickness	37
Strength Equation	42
Beam Strength	47
Effect of Diameter and Wall Thickness	47
Strength Equation	55
LITERATURE CITED	60

THE INSTITUTE OF PAPER CHEMISTRY

Appleton, Wisconsin

STUDY OF FIBER TUBE AND CORE PERFORMANCE

SUMMARY

The objective of this phase of the study was to investigate the relationship between tube and core performance and the core dimensions. To this end, cores were fabricated from two core stocks with inside diameters of 1.5, 3, 6, and 10 inches and nominal wall thicknesses of 0.15, 0.27, 0.48, and 0.66 inch. The winding angle was  $68^\circ$  for the 1.5, 3, and 6-inch diameter cores and  $77^\circ$  for the 10-inch cores. The cores were evaluated for axial crush, side crush, and beam strength. The following conclusions were reached:

1. Analysis of data indicated that the structural formulas proposed in Report One did not adequately account for the effect of winding angle, diameter and thickness on axial crush, side crush, and beam strength. Modified equations were statistically derived and are shown at the end of the Summary. Good agreement between observed and predicted values was obtained with the modified equations.

2. Core performance appears to be affected to a greater extent by winding angle than would be expected from the edgewise compression strength measured in the proper orientation relative to the winding angle. This may occur because failure almost invariably occurs along the spiral path defined by ply gaps. In general, for a constant diameter and wall thickness, a lower winding angle (and hence wider ribbon width) gave higher beam strength and axial crush than expected on the basis of edgewise compression strength. Side crush strength decreased with decreased winding angle but not as much as expected on the basis of edgewise compression strength.

The above is based on rather limited evidence because winding angle was not varied systematically in Phases I and II. In fact, only two comparisons of winding angle effect were possible as follows: (a) 3-inch diameter cores made at 58 and 68° wind angle and (b) 1.5, 3, and 6-inch diameter cores made at a 68° angle as compared to 10-inch diameter cores made at a wind angle of 77°.

Winding angle and ribbon width govern the advance of the core during manufacture. Hence, they affect production speed and presumably manufacturing cost. For this reason it is believed that the effect of winding angle and ribbon width core performance should be studied further.

3. Because torque strength was not determined for the Phase II cores it was not possible to check the effect of dimensions on torque strength. The equations (Va, Vb, VI) shown in Report One may be used to estimate torque strength for cores of various dimensions. However, it appears likely that, for best agreement with observed torque strength, modifying factors should be introduced as for axial crush, etc.

4. With regard to the placement of "high" and "low" strength stocks in the core wall it is believed that the maximum effect would be observed in the case of side crush. Placement of the high strength plies near the outside should give higher side crush strength than the reverse arrangement. Beam strength may also be improved with the "high" strength plies on the outside, although the effect would probably be less than on side crush. Work in this area may be of interest to the group.

5. The above equations do not take into account such factors as fabrication quality, type or amount of adhesive, etc. Such factors may affect strength and should be considered as candidate subjects for future work.

6. The approximate equation derived in Report One [Equation (100), page 141, Ref. (1)] to estimate core stock modified ring strength at intermediate angles based on strength in the M.D. and C.D. was further tested and found to be reasonably accurate. Estimates from the equation were compared with test data at 13, 22, 30, 60, 68, and 77° from the core stock M.D., and the average prediction errors were found to be 4.5 and 3.4% for core stocks A and B, respectively.

The equation is as follows:

$$\frac{1}{\Gamma^2} = \frac{\cos^2 \gamma}{X^2} + \frac{\sin^2 \gamma}{Y^2}$$

where  $\Gamma$  = modified ring strength at  $\gamma$  degrees from the M.D., lb./in.

$X$  = modified ring strength at the M.D., lb./in.

$Y$  = modified ring strength at the cross-machine direction, lb./in.

$\gamma$  = angle from the M.D., degree

a. Axial crush

$$P_a = \frac{\pi (D_o^2 - D_i^2) P_{m\alpha}}{4h_c} [-0.03116 + (0.03573)D_i + (0.24916)(n+1)h_c + (1.45741) \cos \alpha]$$

The average prediction error<sup>a</sup> was 7.02%

b. Beam strength

$$P_b = \frac{\pi (D_o^4 - D_i^4) P_{m\alpha}}{8L D_o h_c} [0.45540 - (0.00717) L/D_i + (0.49133)(n+1)h_c + (0.00184) L + (1.28887) \cos \alpha]$$

The average prediction error<sup>a</sup> was 5.78%

---

<sup>a</sup>See next page for footnote.

c. Side crush

$$P_s = \frac{1.398 N P_{m\theta}}{\left(1 + \frac{D_i}{(N)h_c}\right)\left(1 - \frac{2}{N}\right)} \left[ -0.04033 + (0.08236)D_i - (0.66127)(n + 1)h_c + (1.62042) \cos \alpha \right]$$

The average prediction error<sup>a</sup> was 8.38%

<sup>a</sup>Based on observed values for Phase I and II as reference.

$\underline{P}_a$  = axial crush, lb.

$\underline{P}_{m\alpha}$ ,  $\underline{P}_{m\theta}$  = modified ring compression strength at  $\alpha$  and  $90 - \alpha$  degrees, respectively, lb./in.

$\underline{P}_b$  = beam strength, lb.

$\underline{P}_s$  = side crush, lb./in.

$\alpha$  = angle of wind, degree

$\underline{D}_i$  = inside core diameter, in.

$\underline{D}_o$  = outside diameter, in.

$$= \underline{D}_i + 2(\underline{n} + 1)\underline{h}_c$$

$\underline{N} = \underline{n} + 1$  = effective number of core stock plies

$\underline{n}$  = number of core stock plies

$\underline{t}$ ,  $\underline{h}_c$  = core wall thickness and core stock thickness, respectively, in.

$\underline{L}$  = beam span, in.

## INTRODUCTION

This project is directed to the study of (a) spiral wound tube and core performance, and (b) the development of relationships between spiral wound tube and core performance and the properties of the base stocks and dimensions. The first phase of the study investigated relationships between tube and core performance and the properties of the core stocks. The results obtained are summarized in Report One, dated March 24, 1971 (1).

The second phase of the study is directed toward evaluating the effect of tube and core dimension on core performance. Cores were fabricated having inside diameters of 1.5, 3, 6, and 10 inches. At each diameter the cores were fabricated with nominal wall thicknesses of 0.15, 0.27, 0.48, and 0.66 inch. Core stocks from two different manufacturers were employed. The results obtained are summarized herein.

A review of the literature pertaining to the effect of material properties and core dimensions is contained in Reference (1). In addition, a review of the structural aspects of the various core performance tests is also contained in the same reference.

Generally, tubes are used to protect an enclosure, whereas cores are used to give support to something wrapped around them. However, they are basically the same in a structural sense; therefore, in this report the terms are used interchangeably.

As in the case of the first phase, the cores for this study were fabricated using the same nominal inner and outer liners. Inasmuch as the

liners were essentially a constant factor, their contribution has been approximated in formulating relationships between core tests, core geometry and core stock properties.

It has been assumed that to a first approximation, the core liners were one-half as thick but otherwise identical to the particular core stock being used.

### MATERIALS

Two 0.030-inch core stock samples were obtained for this phase. As set forth in the project proposal, one sample was selected so as to represent higher than average strength (but not extreme) and the other was selected to represent lower than average strength (also not extreme). The sample identifications are shown below:

Sample Code	Report One Identification (Run)	No. of Parent Rolls	Description
A	15	14	Lower than average strength
B	9	9	Higher than average strength

The above samples were manufactured at the time the Phase I samples were made. Standard inner and outer liners (0.014 in.) supplied by the Appleton Manufacturing Company were used in fabricating the cores.

### CORE DIMENSIONS AND CONSTRUCTION

The nominal core dimensions are shown in Table I.

The ribbon widths were selected to maintain a constant winding angle for the 1.5, 3, and 6-inch diameter cores. Because the winder used was limited to 7-inch wide ribbon reels, it was necessary to use a winding angle of 77° in the case of the 10-inch diameter cores.

TABLE I  
NOMINAL CORE DIMENSIONS AND CONSTRUCTION

Inside Diameter, in.	Wall Thickness, in.	No. of Core Stock Plies <sup>a</sup>	Inner Ribbon Width, in.	Inner Ply Winding Angle, degree <sup>b</sup>
1.5	0.15	4	1.75	68
3	0.15	4	3.5	68
6	0.15	4	7.0	68
10	0.15	4	7.0	77
1.5	0.27	8	1.75	68
3	0.27	8	3.5	68
6	0.27	8	7.0	68
10	0.27	8	7.0	77
1.5	0.48	15	1.75	68
3	0.48	15	3.5	68
6	0.48	15	7.0	68
10	0.48	15	7.0	77
1.5	0.66	21	1.75	68
3	0.66	21	3.5	68
6	0.66	21	7.0	68
10	0.66	21	7.0	77

<sup>a</sup>0.015-In. inner and outer liners used for all combinations.

<sup>b</sup>Measured from longitudinal axis.

#### FABRICATION PROCEDURES

The parent rolls were slit into ribbon reels at the Appleton Manufacturing Company. At the time of slitting, full roll width samples were obtained at start and end of each parent roll by Institute personnel. Table II and III show the ribbon reel widths cut for each construction.

The 3, 6, and 10-inch diameter cores were fabricated at the Appleton Manufacturing Company. Attempts to fabricate the 1-1/2-inch diameter cores at Appleton Manufacturing Company were unsuccessful and they were fabricated at a later date by the Sonoco Products Company. However, because of a material

shortage, it was not possible to fabricate the 0.66 wall thickness cores (1-1/2-inch diameter) from core stock B.

TABLE II  
 RIBBON REEL WIDTHS FOR 1.5 AND 3-INCH DIAMETER CORES

Ply	Ribbon Reel Width, in.							
	1.5-In. Diameter				3-In. Diameter			
	0.66 in.	0.48 in.	0.27 in.	0.15 in.	0.66 in.	0.48 in.	0.27 in.	0.15 in.
IL	1-3/4	1-3/4	1-3/4	1-3/4	3-1/2	3-1/2	3-1/2	3-1/2
1	"	"	"	"	"	"	"	"
2	"	"	"	"	"	"	"	"
3	"	"	"	1-1/16	"	"	"	"
4	"	"	"	1-29/32	"	"	"	3-17/32
5	"	"	"	"	"	"	"	"
6	"	"	1-13/16	"	"	"	"	"
7	"	"	1-29/32	"	"	"	3-17/32	"
8	"	"	1-15/16	"	"	"	3-9/16	"
9	"	"	"	"	"	"	"	"
10	"	"	"	"	"	"	"	"
11	"	"	"	"	"	"	"	"
12	"	1-13/16	"	"	"	"	"	"
13	"	1-7/8	"	"	"	3-17/32	"	"
14	"	1-29/32	"	"	"	3-9/16	"	"
15	"	1-15/16	"	"	"	3-19/32	"	"
16	"	"	"	"	"	"	"	"
17	1-13/16	"	"	"	3-17/32	"	"	"
18	1-7/8	"	"	"	3-9/16	"	"	"
19	1-29/32	"	"	"	3-19/32	"	"	"
20	1-15/16	"	"	"	3-5/8	"	"	"
21	1-31/32	"	"	"	3-21/32	"	"	"
OL	2	1-31/32	1-31/32	1-15/16	1-29/32	3-5/8	3-19/32	3-9/16

IL and OL denote Inner and Outer Liner, respectively.

TABLE III

RIBBON REEL WIDTHS FOR 6 AND 10-IN. DIAMETER CORES

Ply	Ribbon Reel Width, in.							
	6-In. Diameter				10-In. Diameter			
	0.66 in.	0.48 in.	0.27 in.	0.15 in.	0.66 in.	0.48 in.	0.27 in.	0.15 in.
IL	7	7	7	7	7	7	7	7
1	"	"	"	"	"	"	"	"
2	"	"	"	"	"	"	"	"
3	"	"	"	"	"	"	"	"
4	"	"	"	7-1/32	"	"	"	7-1/32
5	"	"	"	"	"	"	"	"
6	"	"	"	"	"	"	"	"
7	"	"	7-1/32	"	"	"	7-1/32	"
8	"	"	7-1/16	"	"	"	7-1/16	"
9	"	"	"	"	"	"	"	"
10	"	"	"	"	"	"	"	"
11	"	"	"	"	"	"	"	"
12	"	"	"	"	"	"	"	"
13	"	7-1/32	"	"	"	"	"	"
14	"	7-1/16	"	"	"	7-1/32	"	"
15	"	7-3/32	"	"	"	7-1/16	"	"
16	"	"	"	"	"	"	"	"
17	7-1/32	"	"	"	"	"	"	"
18	7-1/16	"	"	"	"	"	"	"
19	7-3/32	"	"	"	"	"	"	"
20	7-1/8	"	"	"	7-1/32	"	"	"
21	7-5/32	"	"	"	7-1/16	"	"	"
OL	7-3/16	7-1/8	7-3/32	7-1/16	7-3/32	7-3/32	7-3/32	7-1/16

IL and OL denote Inner and Outer Liner, respectively.

The mandrel diameters used were as follows:

Nominal Inside Diameter, in.	Diameter, in.
1.5	--
3	3.015
6	6.015
10	10.015

All cores were fabricated using PVA adhesive (Corn Products No. 8901).  
The solids content was about 12%.

Moisture content samples were obtained at the end of each run on the 3, 6, and 10-inch diameter cores. These samples were weighed and subsequently preconditioned at 10% R.H., 73°F., until equilibrium was attained. They were then conditioned at 50% R.H., 73°F., to equilibrium and oven dried to determine moisture contents. The results are shown in Table IV.

Approximately forty to fifty 80-inch cores were obtained for each combination except in a few instances where difficulties were encountered in the winding operation.

Samples of the inner and outer liners were obtained during the runs.

Difficulties were encountered during the winding operation for the 10-inch diameter cores and to a lesser extent for the 6 and 3-inch diameter cores. Greater difficulties were encountered in winding cores using core stock B than the core stock A. In the thicker wall constructions, particularly frequent stops due to ply breakage and motor throw-outs due to high power consumption made it difficult to achieve steady-state operation and uniformly good adhesion between

TABLE IV

MOISTURE CONTENT OF SPECIMENS TAKEN  
IMMEDIATELY AFTER FABRICATION RUNS

Sample Code	Core Diameter, in.	Wall Thickness, in.	Moisture Content, % o.d.		
			After Winder	After Preconditioning at 10% R.H., 73°F.	After Conditioning at 50% R.H., 73°F.
A	10	0.150	14.2	4.7	9.2
A	10	0.270	16.4	3.9	8.6
A	10	0.480	19.4	3.8	9.0
A	10	0.660	18.9	4.2	8.6
B	10	0.150	12.2	3.5	8.2
B	10	0.270	15.0	4.2	9.0
B	10	0.480	--	4.1	9.0
B	10	0.660	18.4	4.3	9.0
A	6	0.150	15.1	3.3	8.1
A	6	0.270	16.8	4.5	9.2
A	6	0.480	18.2	4.3	9.1
A	6	0.660	19.3	4.1	8.6
B	6	0.150	15.1	3.3	8.2
B	6	0.270	16.4	4.5	9.2
B	6	0.480	17.0	4.8	9.0
B	6	0.660	17.5	4.4	8.9
A	3	0.150	15.9	3.5	8.3
A	3	0.270	15.4	4.3	8.7
A	3	0.480	15.9	4.4	8.9
A	3	0.660	16.9	4.1	8.8
B	3	0.150	--	--	--
B	3	0.270	14.2	3.4	8.2
B	3	0.480	12.0	4.7	9.4
B	3	0.660	16.1	4.1	8.7

plies. During storage it was observed that severe circumferential blisters developed on many of the 10-inch diameter, 0.66-in. wall thickness cores made from core stock B. Observations during test indicate that many of the 10-inch diameter cores made from core stock B exhibited evidence of poor ply adhesion. This also occurred, but to a lesser extent, in the case of the 10-inch diameter (0.15 and 0.27 in. thick) cores made from stock A.

It should also be mentioned that inadvertently the 10-inch diameter, 0.15-inch wall thickness cores made from core stock B were made with five plies of core stock rather than four plies.

### CONDITIONING

The cores were preconditioned at less than 25% R.H., 73°F., and then conditioned at  $50 \pm 2\%$  R.H., 73°F., for at least 30 days prior to test. Selected cores were weighed at periodic intervals during the conditioning period to check the adequacy of the conditioning period. Figure 1 shows data obtained during the conditioning of the 1.5-inch diameter cores at 50% R.H. and indicates the cores reached equilibrium with the conditioning atmosphere in the 30-day period.

The core stock and liner samples were preconditioned for at least 24 hours at  $50 \pm 2\%$  R.H., 73°F., prior to test.

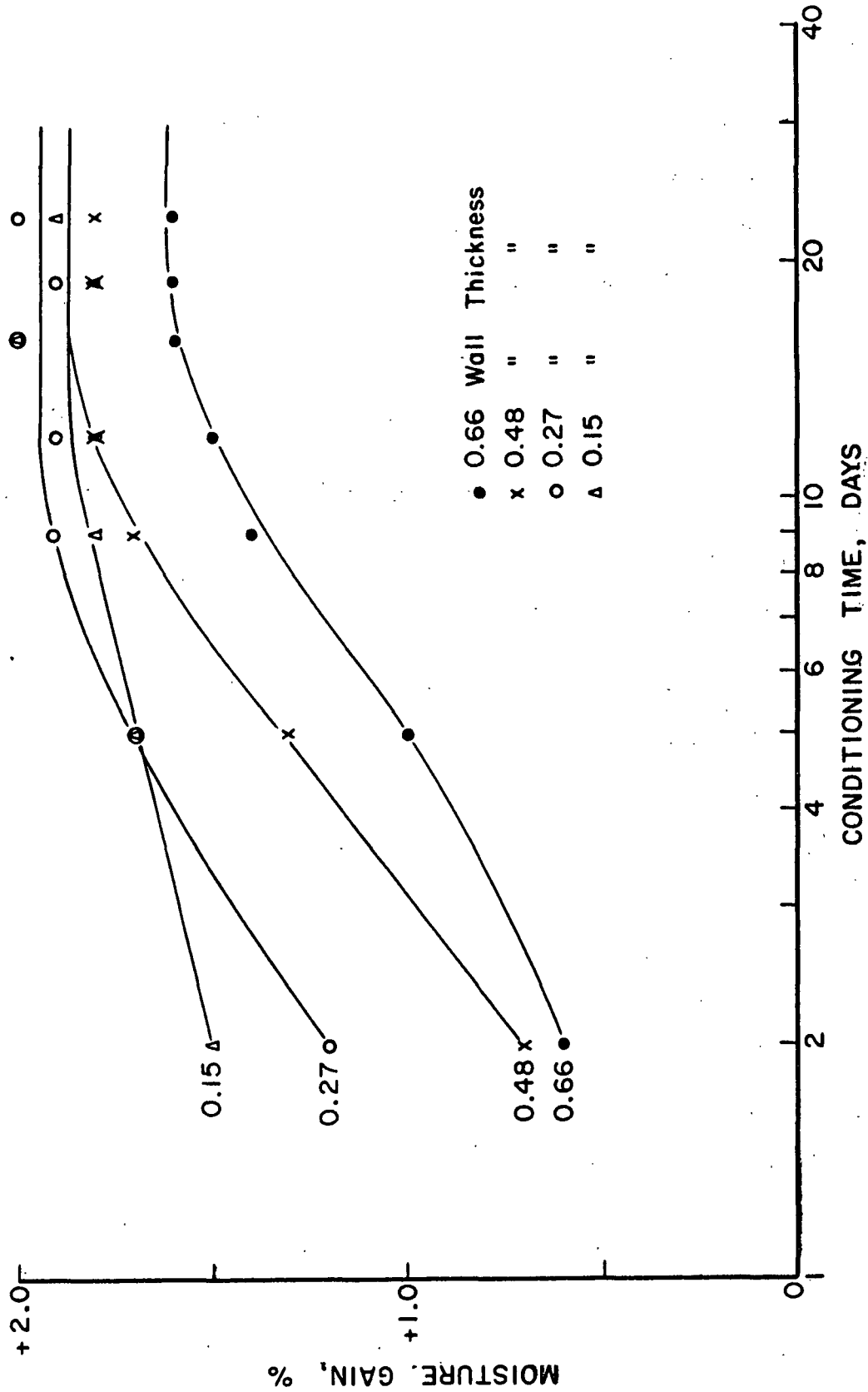


Figure 1. Moisture Gain During Conditioning Period for 1.5-Inch Diameter Cores

## TEST PROCEDURES

### CORE TESTS

The tests carried out on the cores are listed in Table V. In general, NFCTA test procedures were employed. However, for the axial crush tests it was necessary to reduce the test rates to the following to avoid exceeding the rate of load response of the test machine:

1. 1-1/2-in. diameter, 0.66-in. wall thickness: 0.15 in./min.;
2. all other core sizes: 0.2 in./min. (same as in Report One).

To prepare the axial crush specimens, the same procedure used in Report One was employed for the 1-1/2, 3, and 6-inch diameter cores (except 0.66-inch wall thickness) as follows:

1. The specimens were saw-cut to a length slightly in excess of the 4-inch length specified in CT-107.
2. An aluminum plug of appropriate diameter was then inserted in the specimen.
3. The specimen and plug were then placed in a V-block jig and the loading edges were sanded so as to obtain smooth, flat and parallel edges. A 12-inch diameter vertical disk sander was used. The aluminum plug was removed prior to testing.

In the case of the 10-inch diameter cores (and 0.66-in., 6-inch diameter cores), the specimens were very carefully cut to length. They were then placed on a V-block jig and the edges were lightly sanded using the outer circumference of the vertical sander.

TABLE V  
TESTS ON CORES

Test	No. of Tests	Method
1. Side-to-side crush <sup>b</sup>	16	NFCTA T-108
2. Axial (end-to-end) crush <sup>c</sup>	16	NFCTA T-107
3. End supported beam strength <sup>d</sup>		
(a) 36-inch span	8	NFCTA T-114
(b) 72-inch span	8	NFCTA T-114
4. Wall thickness	32	NFCTA CT-101, Method B
5. Inside diameter	8	NFCTA CT-102, Method B
6. Outside diameter	-- <sup>a</sup>	NFCTA CT-103, Method C
7. Moisture content (at time of test)	3	NFCTA CT-111
8. Weight (4-inch long specimen at time of test)	16	

<sup>a</sup>Calculated from inside diameter and wall thickness.

<sup>b</sup>Test rate was 2 inches per minute.

<sup>c</sup>Test rate was 0.2-inch per minute for all cores except the 1-1/2 diameter, 0.66-inch wall thickness cores when the rate was reduced to 0.15-inch per minute to avoid exceeding the speed of response.

<sup>d</sup>Test rate was 2 inches per minute.

The 10-inch diameter cores when tested as 36-in. beams exhibited excessive distortion at the end supports and near the belt when the central load was applied (see Fig. 2). These results should be viewed with caution for this reason. Also, it was not possible to evaluate the 0.66-inch wall thickness beams in the 10-inch diameter because the strength of the belt or its attachment to the fixture was exceeded.

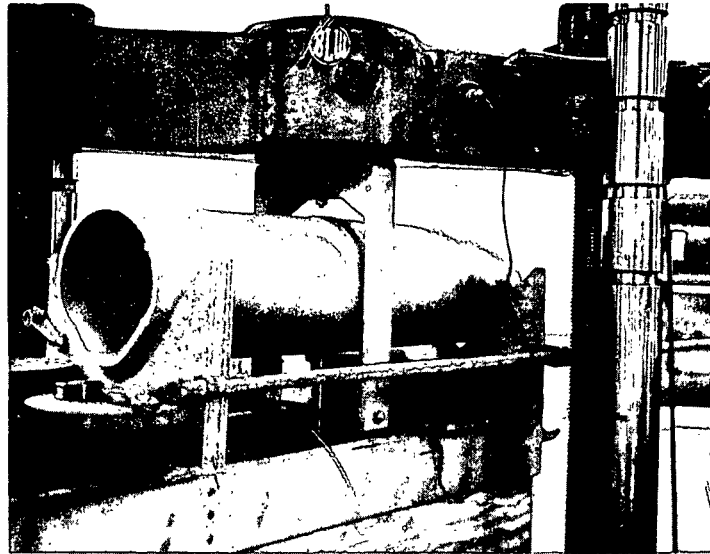


Figure 2. Distortion of 10-Inch Diameter Core in 36-Inch Beam Test

#### CORE STOCK AND LINER TESTS

At time of slitting, full roll width samples were obtained from each parent roll of core stock. The tests carried out on each core stock roll sample are listed in Table VI.

Samples of the inner and outer liners were obtained during the fabrication of the 3, 6, and 10-inch diameter cores. Because of the narrow width (1-3/4 to 2 in.) of the liners for the 1.5-inch diameter cores, no liner samples were obtained. The outer liner samples obtained during fabrication of a given diameter were composited and evaluated as shown in Table VI. The inner liners were treated similarly.

TABLE VI  
TESTS ON CORE STOCK AND LINERS

	Core Stock	Liner Stock
	No. of Tests Per Roll <sup>a</sup>	No. of Tests Per Composite Sample
1. Weight	2000 sq. in.	1000 sq. in.
2. Caliper	12	12
3. Density	--	--
4. Bursting strength	12	12
5. Tensile, stretch and modulus		
M.D.	12	12
C.D.	12	12 <sup>b</sup>
13, 22, 68, 77° to M.D.	12 each	12 <sup>b</sup>
6. Modified ring compression		
M.D.	12	12 <sup>b</sup>
C.D.	12	12 <sup>b</sup>
13, 22, 68, 77° to M.D.	12 each	12 <sup>b</sup>
7. Taber stiffness		
M.D.	12	12
C.D.	12	12
8. Elmendorf tearing strength		
M.D.	12	12
C.D.	12	12
9. TAPPI ply bond	6	6
10. ZDT test	6	6
11. Water drop	6	6
12. Gurley porosity	6	6

<sup>a</sup>Half the tests were made on the sample taken at the start and half on the sample taken at the end of the roll at time of slitting.

<sup>b</sup>Not evaluated on 3-1/2 in. wide liner samples.

## DISCUSSION OF RESULTS

### PROPERTIES OF CORE STOCK AND LINERS

A summary of core stock properties is given in Table VII, while inner and outer liner test results are summarized in Table VIII. Test data for core stock samples taken from each of the several rolls used to fabricate the cores are listed in Table VII. For the purpose of core strength calculations, however, average values of core stock caliper and modified ring compression strength were used for each of the material types. It was felt that this approximation was warranted due to the relatively narrow range between the highest and lowest values for a given core stock type.

In Report One (1), an approximate equation was derived which related the core stock modified ring compression strength at an intermediate angle to those for the machine- and cross-machine directions of the stock [Equation (100), page 141, Ref. (1)]. That equation is the following:

$$\frac{1}{\Gamma^2} = \frac{\cos^2 \gamma}{X^2} + \frac{\sin^2 \gamma}{Y^2} \quad (1)$$

where  $\Gamma$  = modified ring strength of core stock at an angle of  $\gamma$  degree from M.D., lb./in.

$\gamma$  = angle from core stock M.D.; angle at which modified ring strength  $\Gamma$  is defined, degree

$X$  = modified ring strength of core stock at machine direction, lb./in.

$Y$  = modified ring strength of core stock at cross-machine direction, lb./in.

This equation might be useful if it were too inconvenient to test the core stock at the appropriate intermediate angles. The accuracy of the equation in

TABLE VII  
CORE STOCK PROPERTIES

Roll Code	Basis Weight, 2 lb./M ft.	Caliper, pt.	Density, lb./pt.	Bursting Strength, p.s.i.-g.	Modified Ring Compression, lb./in.						Tearing Strength, g.		Taber Stiffness, g.cm.		Porosity, sec./100 cc.
					13° M.D.	22° M.D.	68° M.D.	77° M.D.	to to	to to	M.D.	C.D.	M.D.	C.D.	
1-A	102.4	33.9	3.0	154	57.5	56.5	50.8	32.2	29.7	29.3	549	647	820	231	52
2-A	100.9	33.2	3.0	152	56.3	55.0	51.3	32.2	30.0	29.3	489	677	808	219	52
3-A	98.0	31.8	3.1	168	58.3	56.3	52.3	33.5	31.8	30.0	480	633	780	217	48
4-A	100.3	32.5	3.1	174	58.2	56.3	51.8	32.5	31.8	29.0	536	689	770	229	50
5-A	101.9	32.9	3.1	158	59.5	54.7	52.8	33.5	31.2	30.7	509	689	805	224	56
6-A	98.1	32.1	3.1	171	58.3	56.0	52.7	33.8	31.7	29.8	488	647	773	217	52
7-A	102.6	33.2	3.1	160	59.7	56.0	53.3	33.3	30.5	30.0	519	685	847	233	56
8-A	104.4	33.0	3.2	163	56.5	56.3	53.0	35.5	31.7	28.7	575	693	818	232	52
9-A	102.4	33.1	3.1	165	57.7	54.7	52.5	33.5	30.5	30.5	528	693	825	231	48
10-A	100.6	32.6	3.1	149	56.7	54.7	51.8	33.0	29.5	28.8	504	671	812	220	56
11-A	100.9	32.6	3.1	171	61.2	57.5	53.0	34.0	31.2	30.7	525	651	798	223	56
12-A	99.6	31.9	3.1	180	57.3	54.3	53.0	33.3	30.7	29.5	500	675	760	216	56
13-A	98.2	32.5	3.0	160	56.7	56.5	53.5	34.0	30.7	29.5	493	661	823	206	50
14-A	101.1	33.6	3.0	159	60.5	54.7	53.0	32.3	29.8	29.3	477	616	842	227	48
AV.	100.8	32.8	3.1	163	58.2	55.6	52.5	33.5	30.8	29.6	512	666	806	225	52
1-B	105.7	31.9	3.3	166	67.7	65.3	62.5	40.3	38.3	36.5	543	725	928	261	76
2-B	106.2	31.8	3.3	162	66.7	64.0	60.2	39.2	37.2	36.0	567	717	934	255	80
3-B	107.7	32.2	3.3	165	69.8	62.0	61.3	42.5	40.3	38.8	548	747	934	264	70
4-B	106.7	31.6	3.4	196	72.3	64.0	61.8	44.3	41.7	41.2	535	737	920	272	82
5-B	105.7	31.3	3.4	189	71.8	66.3	63.7	43.8	41.3	40.8	541	695	831	279	70
6-B	107.0	32.2	3.3	169	67.7	63.0	63.2	42.8	39.7	38.3	547	705	946	265	66
7-B	103.4	32.1	3.2	155	65.7	61.7	59.2	38.2	35.5	33.8	528	699	907	254	64
8-B	108.4	31.9	3.4	175	69.3	61.8	61.8	44.0	41.5	39.7	551	727	907	277	64
9-B	105.5	32.4	3.3	167	67.0	62.8	60.3	40.8	38.0	36.3	559	708	958	258	76
AV.	106.3	31.9	3.3	172	68.7	63.4	61.6	41.8	39.3	37.9	547	718	918	265	72

TABLE VII (Continued)  
CORE STOCK PROPERTIES

Roll Code	TAPPI Plybond, P.s.i.g.	ZDT Test p.s.i.	Water Drop, sec.	Baldwin Tensile, lb./in.						Baldwin Stretch, %						Tensile Modulus, p.s.i. (x 10 <sup>-3</sup> )									
				22°		68°		77°		13°		22°		68°		77°		13°		22°		68°		77°	
				M.D.	M.D.	M.D.	M.D.	M.D.	M.D.	M.D.	M.D.	M.D.	M.D.	M.D.	M.D.	M.D.	M.D.	M.D.	M.D.	M.D.	M.D.	M.D.	M.D.	M.D.	M.D.
1-A	120	58	83	165.0	143.3	116.5	48.5	43.8	43.8	1.6	1.8	1.9	3.2	3.3	3.7	523	490	413	157	174	143	153			
2-A	120	59	60	169.2	143.2	118.5	49.7	45.7	45.5	1.7	1.7	2.0	3.4	3.7	3.5	533	497	426	163	149	149	156			
3-A	125	64	32	175.3	149.9	122.0	51.8	47.5	44.8	1.9	2.0	2.2	3.7	4.0	3.7	584	519	442	174	161	161	162			
4-A	129	60	57	175.4	147.3	122.7	52.3	47.9	46.0	1.9	2.0	2.2	3.7	4.0	4.0	576	488	436	170	159	159	159			
5-A	128	60	82	170.8	142.2	114.2	47.9	43.2	42.7	1.7	1.8	1.9	3.1	3.3	3.3	570	488	428	164	147	147	150			
6-A	132	64	30	171.8	147.3	118.7	50.6	47.2	44.8	1.9	2.1	2.1	3.4	4.0	3.6	562	487	435	174	158	158	165			
7-A	114	59	65	174.1	148.4	120.0	50.0	46.1	45.2	1.8	1.9	2.0	3.3	3.5	3.7	562	497	427	161	147	147	149			
8-A	126	58	70	170.8	151.2	121.7	49.8	46.2	45.6	1.7	2.0	2.0	3.0	3.6	3.6	563	517	442	166	155	155	156			
9-A	127	60	70	175.7	148.6	118.3	49.6	46.6	45.0	1.8	1.9	2.0	3.2	3.8	3.5	564	511	432	159	149	149	154			
10-A	125	58	84	170.5	140.4	114.7	47.8	42.0	42.5	1.7	1.8	1.8	3.4	3.1	3.5	582	510	440	159	146	146	151			
11-A	131	63	43	177.5	151.5	126.8	51.2	47.4	45.6	1.8	2.1	2.2	3.4	3.8	3.9	566	501	461	172	158	158	161			
12-A	132	64	62	176.4	147.0	120.4	50.4	46.7	45.5	1.9	2.2	2.2	3.5	3.7	3.8	555	498	446	169	156	156	157			
13-A	129	65	28	167.7	147.3	124.2	52.3	47.6	45.4	1.8	1.9	2.1	3.8	3.7	4.0	562	512	470	169	153	153	171			
14-A	121	59	104	166.3	140.2	115.9	47.7	43.5	42.4	1.7	1.7	1.8	3.2	3.3	3.3	544	488	438	159	142	142	156			
AV.	126	61	62	171.9	146.3	119.6	50.0	45.8	44.5	1.8	1.9	2.0	3.4	3.6	3.6	560	500	438	165	152	152	157			
1-B	132	70	36	191.1	174.9	144.7	54.1	49.2	47.3	1.5	1.7	1.9	3.1	3.2	3.1	675	640	522	192	179	179	184			
2-B	130	66	262	183.0	164.8	134.9	52.3	47.9	46.1	1.5	1.5	1.6	2.8	3.0	3.0	650	623	519	190	179	179	178			
3-B	132	69	29	190.2	175.5	147.9	56.9	51.6	49.1	1.5	1.6	1.8	2.9	2.9	3.2	646	669	531	204	195	195	186			
4-B	153	77	88	212.9	179.9	153.2	59.7	55.2	53.3	1.8	1.7	1.9	2.8	3.1	3.3	685	664	548	218	204	204	208			
5-B	146	78	107	201.5	185.2	152.2	58.6	52.8	52.4	1.8	1.9	2.0	3.0	3.0	3.0	657	651	544	208	195	195	204			
6-B	124	72	24	195.0	175.0	144.7	56.8	48.0	49.7	1.6	1.7	1.8	2.8	3.0	3.0	659	637	530	206	184	184	194			
7-B	138	65	416	167.9	163.1	131.2	51.2	49.6	44.3	1.3	1.5	1.6	2.6	2.9	2.8	626	634	510	194	195	195	175			
8-B	137	72	27	193.0	173.2	144.1	58.0	53.0	50.2	1.6	1.6	1.8	2.8	3.2	3.0	661	644	529	213	202	202	195			
9-B	136	70	49	187.7	169.5	142.1	54.1	49.1	46.5	1.5	1.6	1.8	2.9	3.2	3.1	664	639	528	193	184	184	172			
AV.	136	71	115	191.4	173.5	143.9	55.7	50.7	48.8	1.6	1.6	1.8	2.9	3.1	3.1	658	645	529	202	191	191	188			

TABLE VIII  
INNER AND OUTER LINER TEST RESULTS

Test	Inner Liner				Outer Liner			
	3-in.	6-in.	10-in.	Av.	3-in.	6-in.	10-in.	Av.
	D. Cores 7117	D. Cores 7118	D. Cores 7122		D. Cores 7116	D. Cores 7119/20	D. Cores 7121	
Basis wt., lb./M ft. <sup>2</sup>	55.9	57.1	61.6	58.2	58.0	58.6	56.5	57.7
Caliper, pt.	15.3	15.4	15.6	15.4	15.5	15.7	15.8	15.7
Density, lb./pt.	3.7	3.7	3.9	3.8	3.7	3.7	3.6	3.7
Bursting strength, p.s.i.g.	120	120	130	123	121	118	116	118
Mod. ring compression, lb./in., M.D.	31.5 <sup>a</sup>	29.3	29.5	30.1	32.5 <sup>a</sup>	29.0	28.7	30.1
13° to M.D.	-- <sup>a</sup>	29.0	28.8	28.9	-- <sup>a</sup>	28.4	27.8	28.1
22° to M.D.	-- <sup>a</sup>	28.3	28.5	28.4	-- <sup>a</sup>	27.5	27.0	27.2
68° to M.D.	-- <sup>a</sup>	20.3	21.2	20.8	-- <sup>a</sup>	20.4	19.8	20.1
77° to M.D.	-- <sup>a</sup>	18.8	19.7	19.2	-- <sup>a</sup>	18.4	18.0	18.2
C.D.	17.3	17.7	18.7	17.9	21.2	17.4	17.0	18.5
Tearing strength, g., M.D.	193	212	241	215	213	206	203	207
C.D.	388	397	429	405	405	393	397	398
Taber stiffness, g.cm., M.D.	149	158	176	161	156	155	158	156
C.D.	54	44	53	50	47	46	40	44
Porosity, sec./100 cc.	124	114	132	123	114	114	108	112
TAPPI ply-bond, p.s.i.g.	149	149	148	149	148	146	150	148
ZDT test, p.s.i.	76	80	80	79	74	76	79	76
Water drop, sec.	117	107	179	134	111	300	280	230
Tensile, lb./in., M.D.	114.2 <sup>a</sup>	114.1	117.5	115.3	118.3 <sup>a</sup>	111.6	111.1	113.7
13° to M.D.	-- <sup>a</sup>	86.8	97.6	92.2	-- <sup>a</sup>	85.8	81.7	83.8
22° to M.D.	-- <sup>a</sup>	62.9	73.1	68.0	-- <sup>a</sup>	63.2	59.6	61.4
68° to M.D.	-- <sup>a</sup>	22.5	24.3	23.4	-- <sup>a</sup>	21.9	21.4	21.6
77° to M.D.	-- <sup>a</sup>	20.9	22.1	21.5	-- <sup>a</sup>	20.2	19.9	20.0
C.D.	--	20.0	20.8	20.4	--	20.0	19.1	19.6
Stretch, %, M.D.	2.3 <sup>a</sup>	2.1	2.0	2.1	2.3 <sup>a</sup>	2.1	2.2	2.2
13° to M.D.	-- <sup>a</sup>	2.3	2.2	2.2	-- <sup>a</sup>	2.1	2.2	2.2
22° to M.D.	-- <sup>a</sup>	2.5	2.4	2.4	-- <sup>a</sup>	2.3	2.4	2.4
68° to M.D.	-- <sup>a</sup>	4.5	4.9	4.7	-- <sup>a</sup>	4.2	4.6	4.4
77° to M.D.	-- <sup>a</sup>	4.7	4.7	4.7	-- <sup>a</sup>	4.4	4.4	4.4
C.D.	--	5.0	5.0	5.0	--	4.7	4.3	4.5
Tensile modulus, p.s.i. x 10 <sup>-3</sup> , M.D.	737 <sup>a</sup>	745	783	755	755 <sup>a</sup>	727	717	733
13° to M.D.	-- <sup>a</sup>	624	675	650	-- <sup>a</sup>	612	585	598
22° to M.D.	-- <sup>a</sup>	475	530	502	-- <sup>a</sup>	482	452	467
68° to M.D.	-- <sup>a</sup>	150	153	152	-- <sup>a</sup>	142	137	140
77° to M.D.	-- <sup>a</sup>	142	140	141	-- <sup>a</sup>	130	121	126
C.D.	--	136	123	130	--	123	115	119

<sup>a</sup> Not tested because of narrow ribbon width.

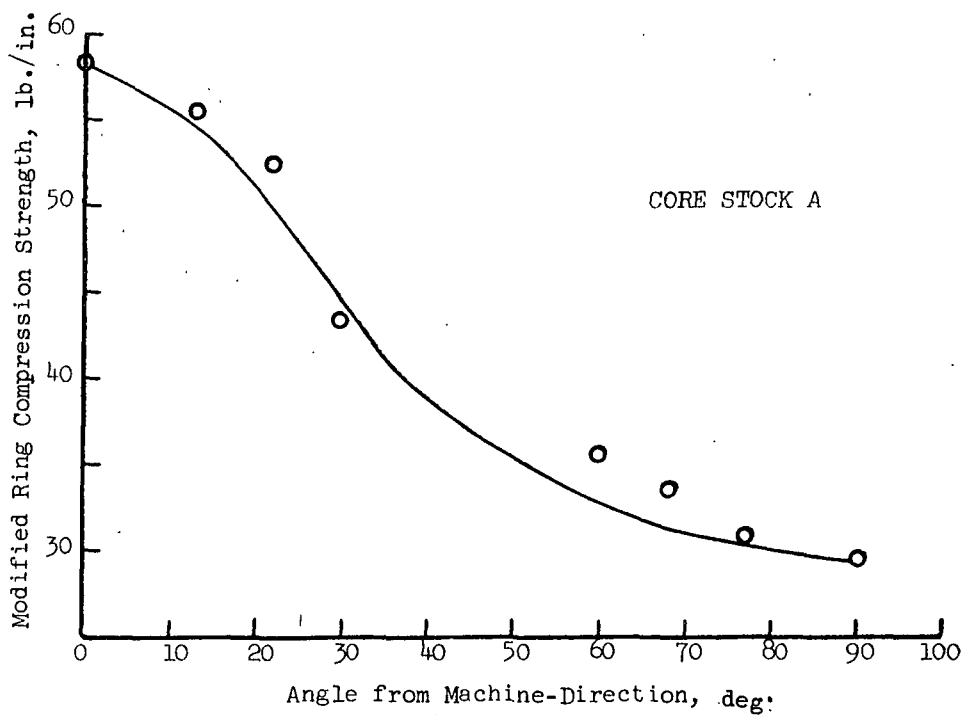
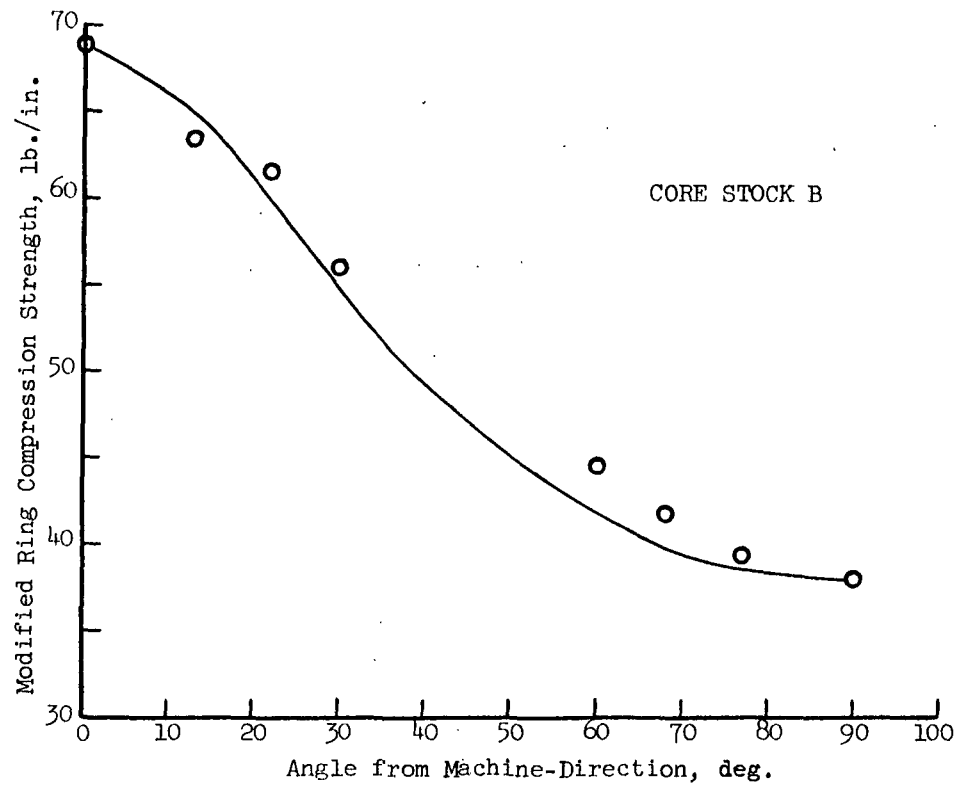


Figure 3. Theoretical and Observed Core Stock Compression Strengths at Intermediate Angles

TABLE IX  
CORE TEST RESULTS FOR CORE STOCK A

Roll Code	Inside Diameter, in.	Wall Thickness, in.	Outside Diameter, in.	Weight, lb.	Moisture Content, % (o.d.)	Side Crush Load, lb./in.	Axial Crush, lb.	Beam Strength, lb.		Beam Stiffness (EI)		True Stiffness
								36-in. Span	72-in. Span	36-in. Span	72-in. Span	
1-A	1.498	0.152	1.802	0.072	8.1	31.2	516	36.8	14.7	5.0	5.1	5.1
2-A	1.498	0.276	2.050	0.138	7.9	59.8	971	70.6	32.4	10.9	11.0	11.1
3-A	1.497	0.481	2.459	0.261	8.1	116.0	2163	175.0	81.6	26.3	28.0	28.6
4-A	1.500	0.656	2.812	0.385	8.2	151.2	2909	252.0	119.3	42.9	51.8	55.6
5-A	3.009	0.148	3.305	0.141	7.9	24.4	1247	151	72	32.4	40.3	43.0
6-A	3.002	0.272	3.546	0.263	8.0	52.0	2482	334	172	64.2	83.3	92.5
7-A	3.006	0.487	3.980	0.488	8.1	97.4	4897	680	338	125.7	163.1	181.1
8-A	3.007	0.660	4.327	0.691	7.9	129.0	6838	992	500	185.1	252.8	287.9
9-A	6.012	0.156	6.324	0.281	7.7	15.7	2291	502	250	181.3	266.9	316.81
10-A	6.011	0.281	6.573	0.524	7.7	37.6	5159	1064	557	334.4	517.5	633.11
11-A	6.017	0.503	7.023	0.967	7.7	80.0	10494	2330	1165	587.3	951.0	1198.36
12-A	6.018	0.690	7.398	1.341	7.9	112.4	14591	3527	1736	730.8	1448.9	2154.68
13-A	10.020	0.153	10.326	0.450	7.8	8.8	2984	974	626	b	718.6	b
14-A	10.003	0.284	10.571	0.826	8.2	25.0	6172	2194	1225	--b	1511.4	--b
15-A	10.011	0.498	11.007	1.482	7.9	59.4	13291	500 <sub>f</sub>	2673	--b	2920.6	--b
16-A	10.009	0.694	11.397	2.123	7.8	93.8	18903	--	4087	--a	3909.2	--a

<sup>a</sup> Beam strength exceeded strength of loading belts.

<sup>b</sup> Not calculated because of excessive distortion of core during test.

Note: Winding angle for 1.5, 3 and 6-in. diameter cores was 68°, whereas winding angle for 10-in. diameter cores was 77°.

TABLE X  
CORE TEST RESULTS FOR CORE STOCK B

Roll Code	Inside Diameter, in.	Wall Thickness, in.	Outside Diameter, in.	Weight, lb.	Moisture Content, % (o.d.)	Side Crush Load, lb./in.	Axial Crush, lb.	Beam Strength, lb.		Beam Stiffness (EI)	
								36-in. Span	72-in. Span	36-in. Span	72-in. Span
1-B	1.497	0.150	1.797	0.077	8.1	39.8	618	41.4	17.6	6.0	6.3
2-B	1.497	0.268	2.033	0.142	8.0	71.2	1324	90.1	39.5	12.4	12.5
3-B	1.498	0.473	2.444	0.280	8.1	132.8	2748	221.0	99.8	29.5	30.0
4-B	3.008	0.146	3.300	0.146	8.0	25.4	1566	182	87	36.6	44.3
5-B	3.004	0.265	3.534	0.269	8.0	53.3	2955	368	176	70.5	92.5
6-B	3.004	0.477	3.958	0.514	8.1	102.0	5931	782	398	149.1	188.2
7-B	3.004	0.649	4.302	0.742	8.0	141.8	8747	1209	601	220.8	291.4
8-B	6.004	0.152	6.308	0.292	7.9	17.2	2801	588	274	216.2	305.5
9-B	6.008	0.274	6.556	0.545	8.1	38.3	6612	1330	682	394.7	620.4
10-B	6.012	0.476	6.964	0.975	8.1	96.9	12916	2818	1406	664.8	1078.5
11-B	6.012	0.663	7.338	1.408	8.2	104.4	18981	4221	2132	882.6	1688.0
12-B	10.011	0.182	10.375	0.580	8.2	14.9	4766	1491	956	b	1101.7
13-B	10.011	0.275	10.561	0.859	8.2	26.0	7403	2664	1511	--b	1641.7
14-B	10.001	0.488	10.977	1.550	8.0	52.7	14144	5479	2944	--b	3223.2
15-B	10.005	0.674	11.353	2.202	8.3	87.3	23228	--	4572	--a	4048.2

<sup>a</sup>Beam strength exceeded strength of loading belts.

<sup>b</sup>Not calculated because of excessive distortion of core during test.

Note: Winding angle for 1.5, 3 and 6-in. diameter cores was 68°, whereas winding angle for 10-in. diameter cores was 77°.

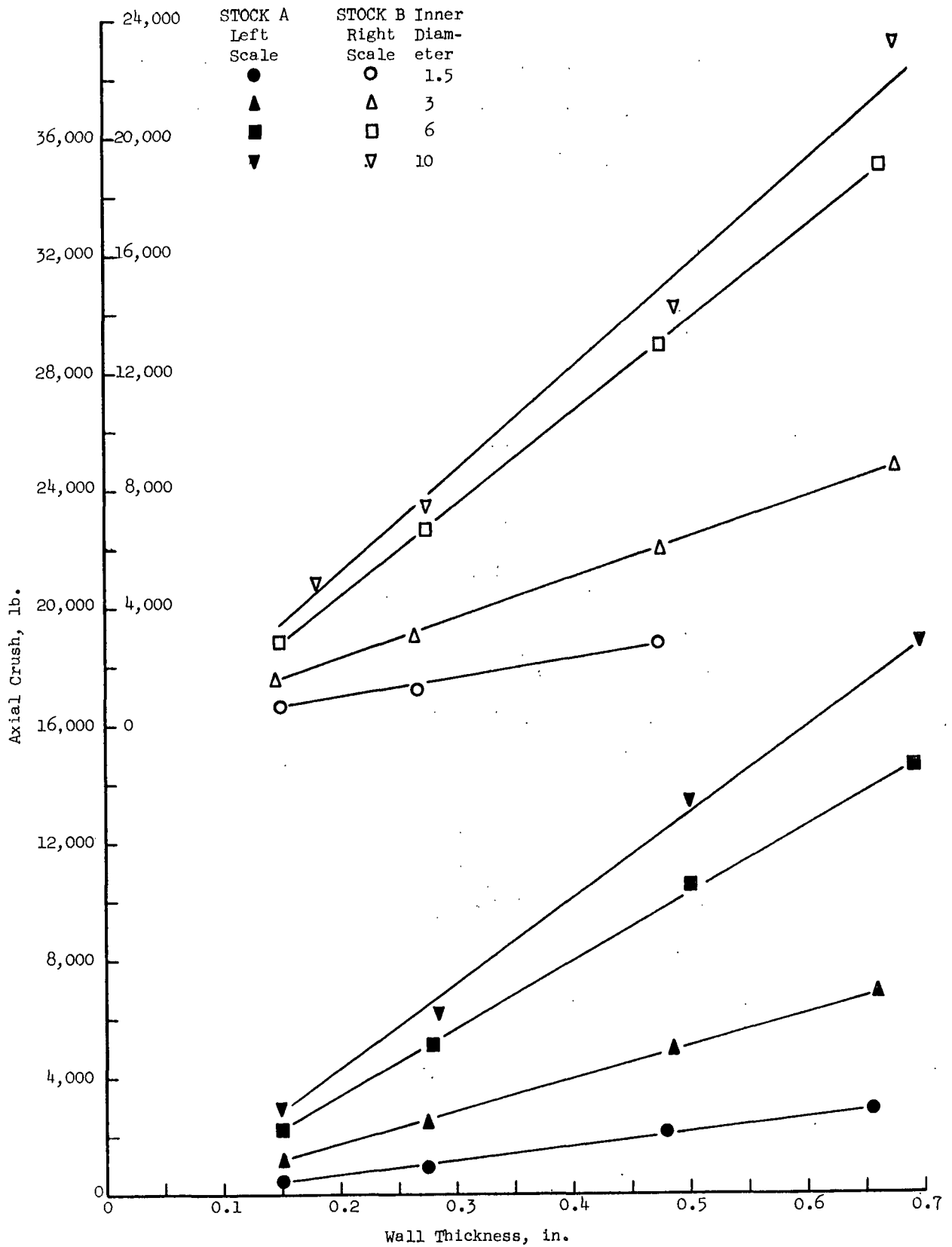


Figure 5. Observed Axial Crush Strength vs. Core Wall Thickness

diameter cores are excluded. Similarly, the trends shown in Fig. 5 indicate that the relationship between axial crush strength and wall thickness is also linear.

In Report One (1) an equation was derived which enables estimation of axial crush strength based on core stock properties and core dimensions, and is as follows [Equation (47), page 91, Ref. (1)]:

$$P_a = \frac{\pi(D_o^2 - D_i^2)}{4h_c} P_{m\alpha} \quad (2)$$

where  $P_a$  = axial crush strength, lb.

$D_o$  = outer core diameter, in.

$D_i$  = inner core diameter, in.

$h_c$  = core stock thickness, in.

$P_{m\alpha}$  = modified ring compression strength of core stock in a direction  $\alpha$  degree from the M.D., lb./in.

$\alpha$  = angle between core stock M.D. and core axial direction;  
angle of wind, degree

Although it is not apparent from the form of this equation, the estimated axial crush strength is linearly related to both the average core diameter and wall thickness. An equivalent form of Equation (2) is the following:

$$P_a = \pi \frac{P_{m\alpha}}{h_c} T D_{av} \quad (3)$$

where  $T = (n + 1)h_c$  = wall thickness, in.

$D_{av} = D_i + T$  = average core diameter, in.

$n$  = number of core stock plies

Although Equation (3) predicts a linear relationship between axial crush strength, average diameter and wall thickness, and the trends shown in Fig. 4 and 5 support that prediction, Equation (3) by itself could not provide adequate estimates of

axial crush strength. This fact is illustrated by Fig. 6 in which the estimated axial crush strength [computed from Equation (3)] is plotted vs. the observed axial crush strength. To provide a common scale for all data, both ordinate and abscissa were divided by a common factor, section area.

The data points in Fig. 6 would all lie on the indicated straight line if Equation (3) were accurate. Unfortunately, not only do the data deviate significantly from the line, but the amount of deviation is dependent on the core diameter and wall thickness. In addition the 10-inch diameter data suggest that an additional factor may be involved, inasmuch as these data violate a clearly indicated trend in the amount of deviation from the line with respect to core diameter.

The only apparent difference between the 10-inch diameter cores and the others from this study, other than the diameter itself, was the winding angle. The 1.5, 3, and 6-inch diameter cores were constructed by winding at  $68^\circ$  while the 10-inch diameter cores were made by winding at  $77^\circ$ . It was suggested, therefore, that increased winding angles may have a deleterious effect on axial core performance. As a test of this hypothesis, the 3-inch diameter cores from Phase I of this study, wound at  $60^\circ$ , were compared with the 3-inch diameter cores of the current phase, wound at  $68^\circ$ . The two sets of cores employed the same core stock, adhesive, number of plies, and manufacturer. The results indicated that the cores wound at  $68^\circ$  were significantly weaker than those wound at  $60^\circ$ . Thus, winding angle was again implicated as a significant factor in determining the axial crush strength of cores.

Statistical analysis of the axial crush data supports the preliminary conclusions reached by inspection of Fig. 6, namely, that core diameter, wall thickness, and winding angle were significant factors which were necessary to

adjust the estimates provided by Equation (3). Lending further support to the significance of these three factors, is the fact that similar adjusting terms were required to obtain accurate estimates of side crush and beam strengths as well.

#### Axial Strength Equation

The final form of the equation to be used in estimating the axial crush strength of cores is as follows:

$$P_a = P_{nom,a} \{-0.03116 + (0.03573) D_i + (0.24916)(n + 1)h_c + (1.45741) \cos \alpha\} \quad (4)$$

where  $P_a$  = axial crush strength, lb.

$$P_{nom,a} = \pi/4 (D_o^2 - D_i^2) P_{m\alpha}/h_c \quad (5)$$

= nominal estimate of axial crush strength, lb.

$$D_o = D_i + 2(n + 1)h_c \quad (6)$$

= outer core diameter, in.

$D_i$  = inner core diameter, in.

$n$  = number of core stock plies

$h_c$  = core stock thickness, in.

$P_{m\alpha}$  = modified ring compression strength of core stock in a direction  $\alpha$  degrees from M.D., lb./in.

$\alpha$  = winding angle; angle between core stock M.D. and core axis, degree

The average error of estimation incurred through the use of Equation (4) when applied to all Phase I and Phase II, data was 7.02%, and the correlation coefficient was 0.847. The correlation is illustrated by Fig. 7 in which the final estimated loads are plotted vs. observed values.

It may be noted that both wall thickness and outer core diameter are defined in terms of the core stock thickness and the number of plies. Thus, the strength of the core may be estimated before manufacture, whereas the use of the measured wall thickness and outer diameter dimensions would require that a finished core be on hand for measurement.

No interpretation can be offered at this time which would adequately explain the necessity for the winding angle correction term. It has been noted, however, that core failure usually occurs along one or more of the spiral ply-gap lines. It may be theorized that, at a winding angle of zero degrees, in which the ply gaps would be parallel with the core axis, the axial load would be parallel with the gap and no load transfer across the gap would be required. On the other hand, at a winding angle of 90 degrees, in which ply gaps would be perpendicular with the core axis and load direction, the entire axial load would have to be transferred across the ply gaps. Thus, at least for the two extremes of all possible winding angles, one might expect that cores wound at higher winding angles would be weaker than those wound at lower angles, even though each strength estimate were based on the core stock strength at the appropriate angle. It becomes less clear, however, exactly why this trend should hold true for angles intermediate between zero and ninety degrees, as it apparently does. Due to the very high significance of the winding angle term, and the paucity of pertinent available data, further work on this subject is indicated.

An explanation for the diameter correction term is even more difficult to offer for the axially loaded cores. The diameter effect is one whereby the axial crush strength is increased as core diameter is increased even though the increase in section area is considered. Further work is indicated to provide a more enlightened understanding of the mechanisms of core failure.

### Side Crush

#### Effect of Diameter and Wall Thickness

The effects of changing core diameter and wall thickness on the strength of cores when loaded in a side-to-side manner are shown in Fig. 8 through 11. The general trends of the data are indicated by straight lines. The graphs utilize logarithmic scales so that if the data appear to lie closely to a straight line a "linear" relationship is not implied. Figures 8 and 9 indicate that as a core's diameter is increased, its strength in side crush is reduced. Figures 10 and 11, on the other hand, show that increasing a core's wall thickness increases its side crush strength. These trends are in line with predictions based on the following equation, which was derived in Report One (1) and which relates side crush strength to core stock properties and core dimensions. [Equation (66), page 121, Ref. (1)]:

$$P_s = \frac{P_{m\theta} t^2}{0.9549 (D_i/t + 1)(t - 2h_l - h_c)h_c} \quad (7)$$

where  $P_s$  = side crush strength of core, lb./in.

$P_{m\theta}$  = modified ring compression strength of core stock at a direction  $\theta$  degree from the M.D., lb./in.

$\theta$  = complement of winding angle; angle between core stock M.D. and core circumferential direction, degree

$t$  = core wall thickness, in.

$D_i$  = inner core diameter, in.

$h_l$  = inner or outer core liner thickness, in.

$h_c$  = core stock thickness, in.

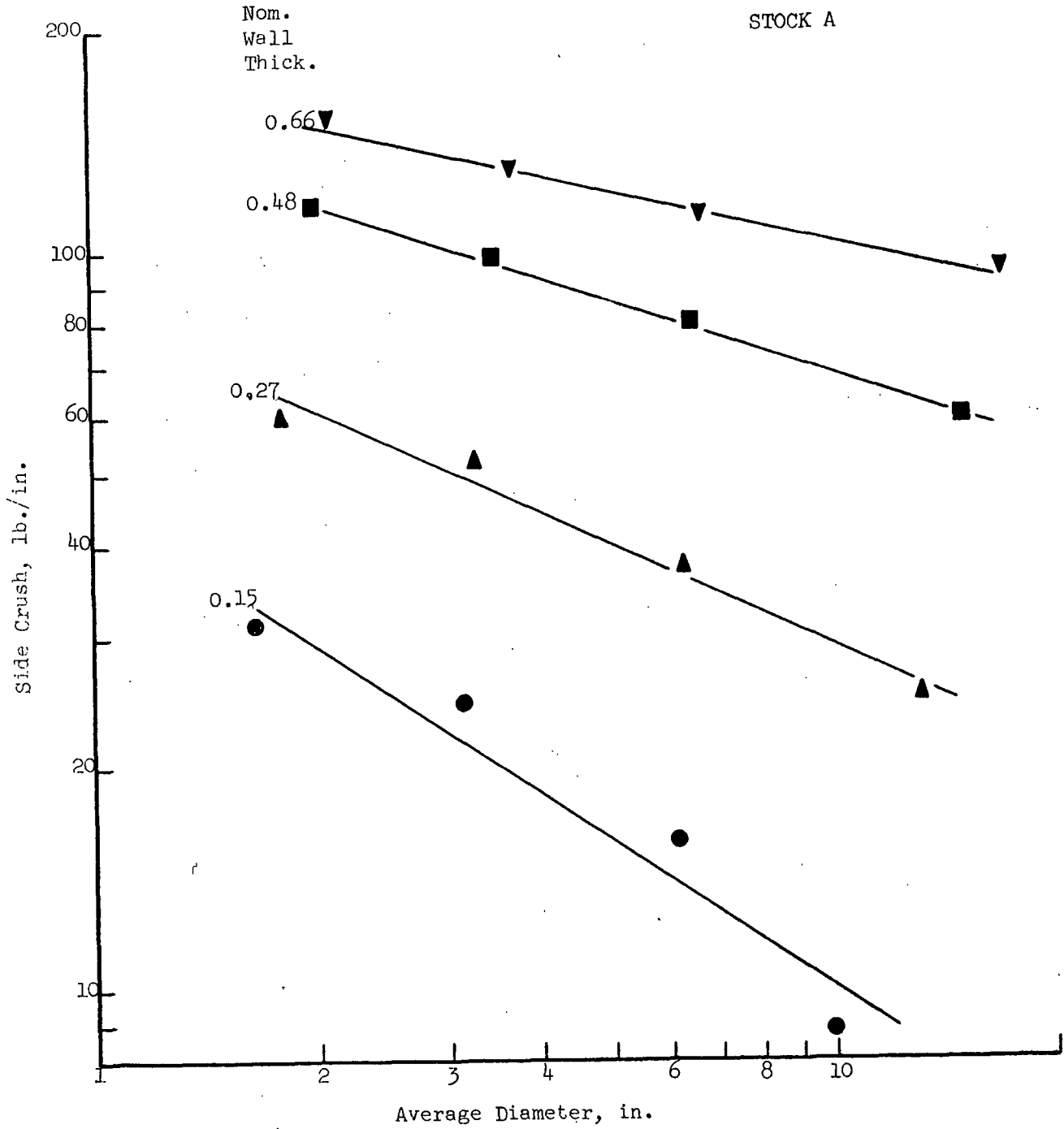


Figure 8. Observed Side Crush Strength vs. Average Core Diameter for Stock A

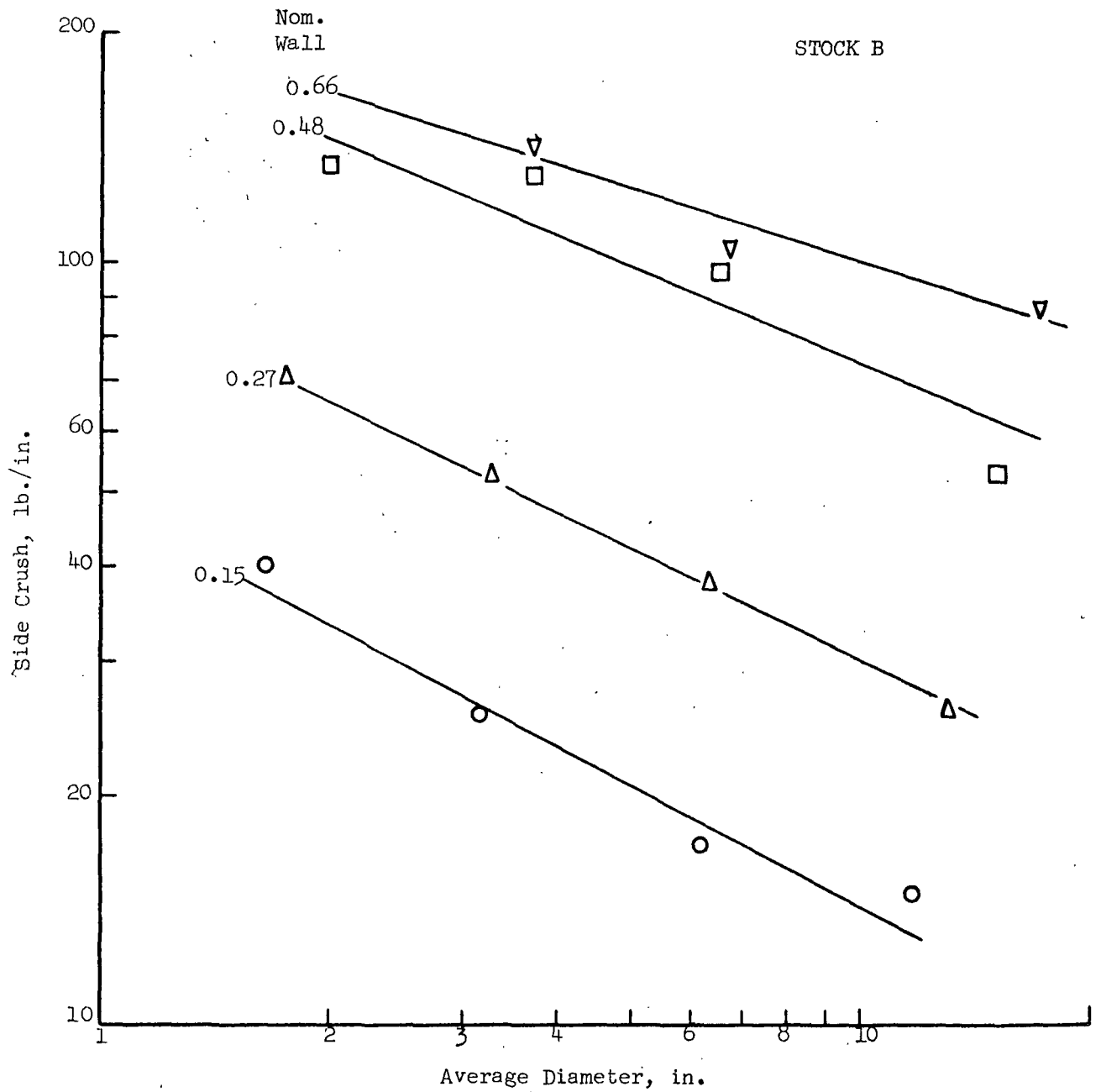


Figure 9. Observed Side Crush Strength vs. Average Core Diameter for Stock B

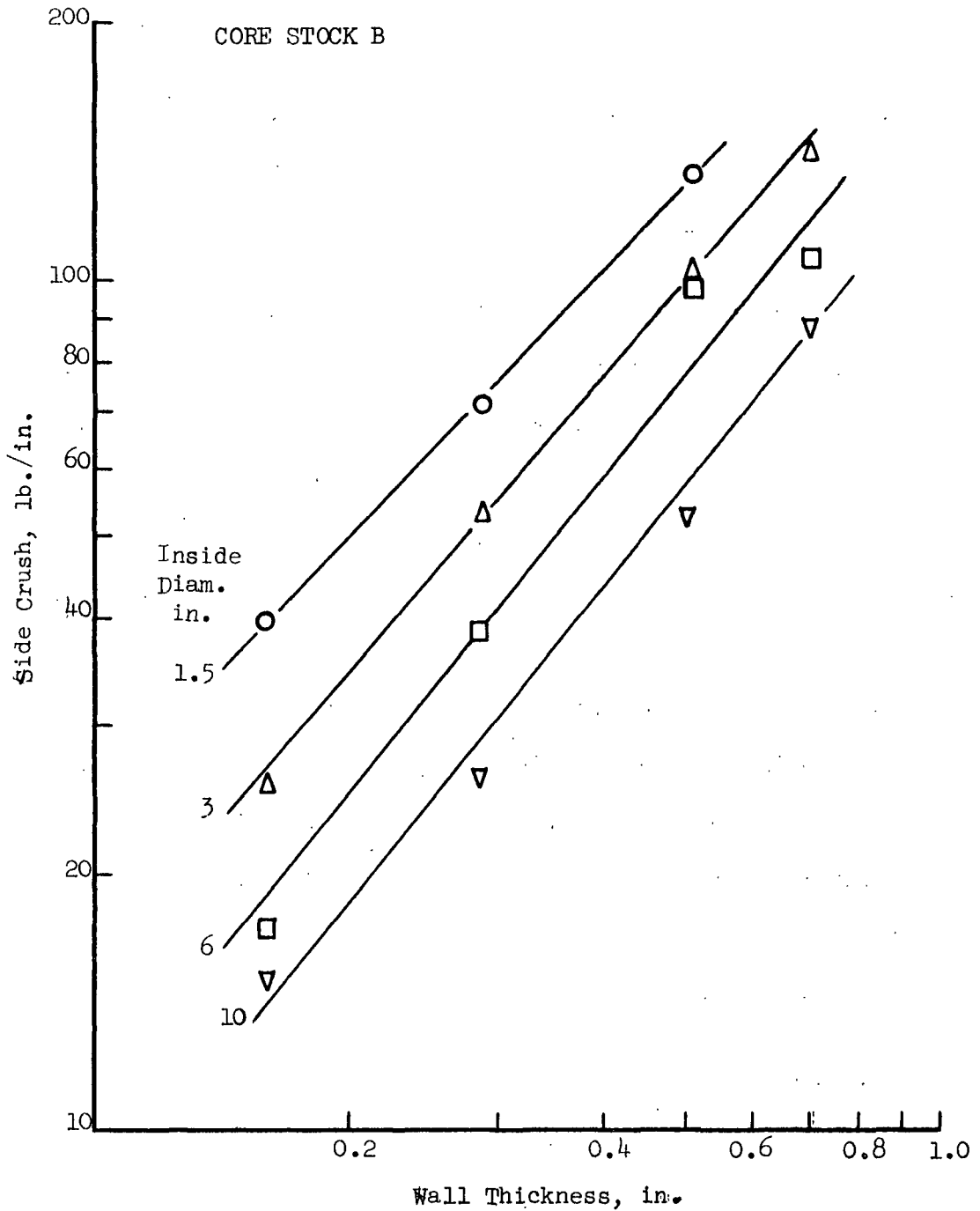


Figure 11. Observed Side Crush Strength vs. Core Wall Thickness for Stock B

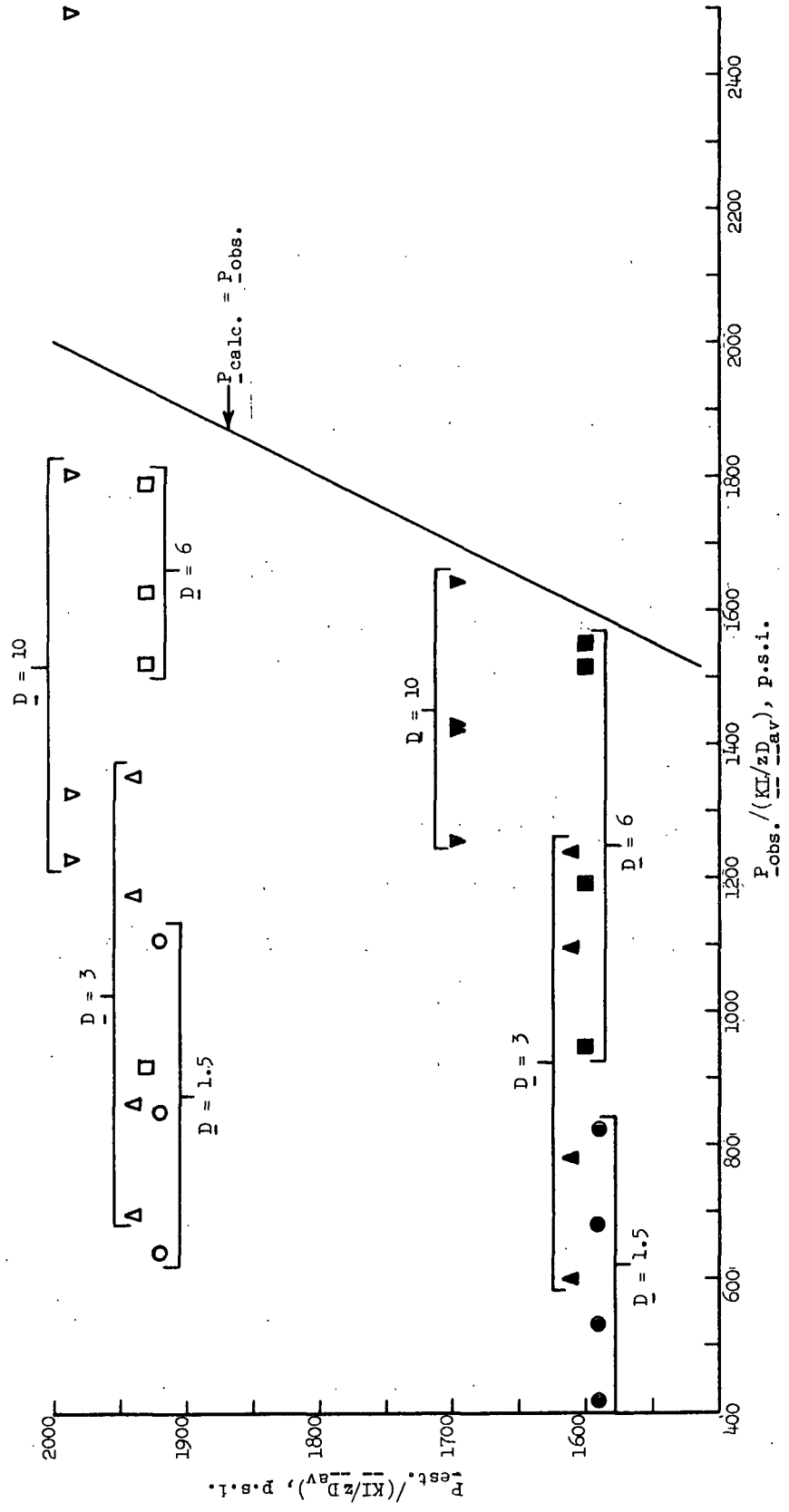


Figure 12. Nominal Estimates of Side Crush Strength vs. Observed Values [Equation (5)]

$$P_s = P_{\text{nom},s} \{-0.04033 + (0.08236) D_i - (0.66127)(n + 1)h_c + (1.62042) \cos \alpha\} \quad (9)$$

where  $P_s$  = side crush strength, lb.

$P_{\text{nom},s}$  = nominal estimation of side crush strength, defined in Equation (8), lb.

The average error of estimation resulting from application of Equation (9) to all the samples from Phases I and II was 8.4% and the correlation coefficient was 0.932. A graph in which the estimates made from Equation (9) were plotted vs. observed values is shown in Fig. 13.

The winding angle adjusting term in Equation (9) implies that an increased winding angle causes a reduction in core strength relative to nominal estimates. As in the case of axial loading, no adequate rationale is available at this time to explain this behavior.

The diameter and wall thickness correction terms in Equation (9) imply that for a given wall thickness and winding angle a decrease in core diameter causes core strength to become less than the nominal estimate [Equation (8)]. And if diameter and winding angle remain constant while wall thickness increases, core strength again becomes less than nominal. Both of these trends - decreasing diameter and increasing wall thickness - tend to move the core geometry away from the thin ring shape which was assumed to exist in the derivation of the nominal equation, Equation (8).

Some of the cores, particularly the small diameter ones, can hardly be considered thin rings. An appreciable deviation from estimates based on thin ring theory is to be expected then. But there is an additional problem involved in analyzing the cores which can be considered thin rings. That problem is

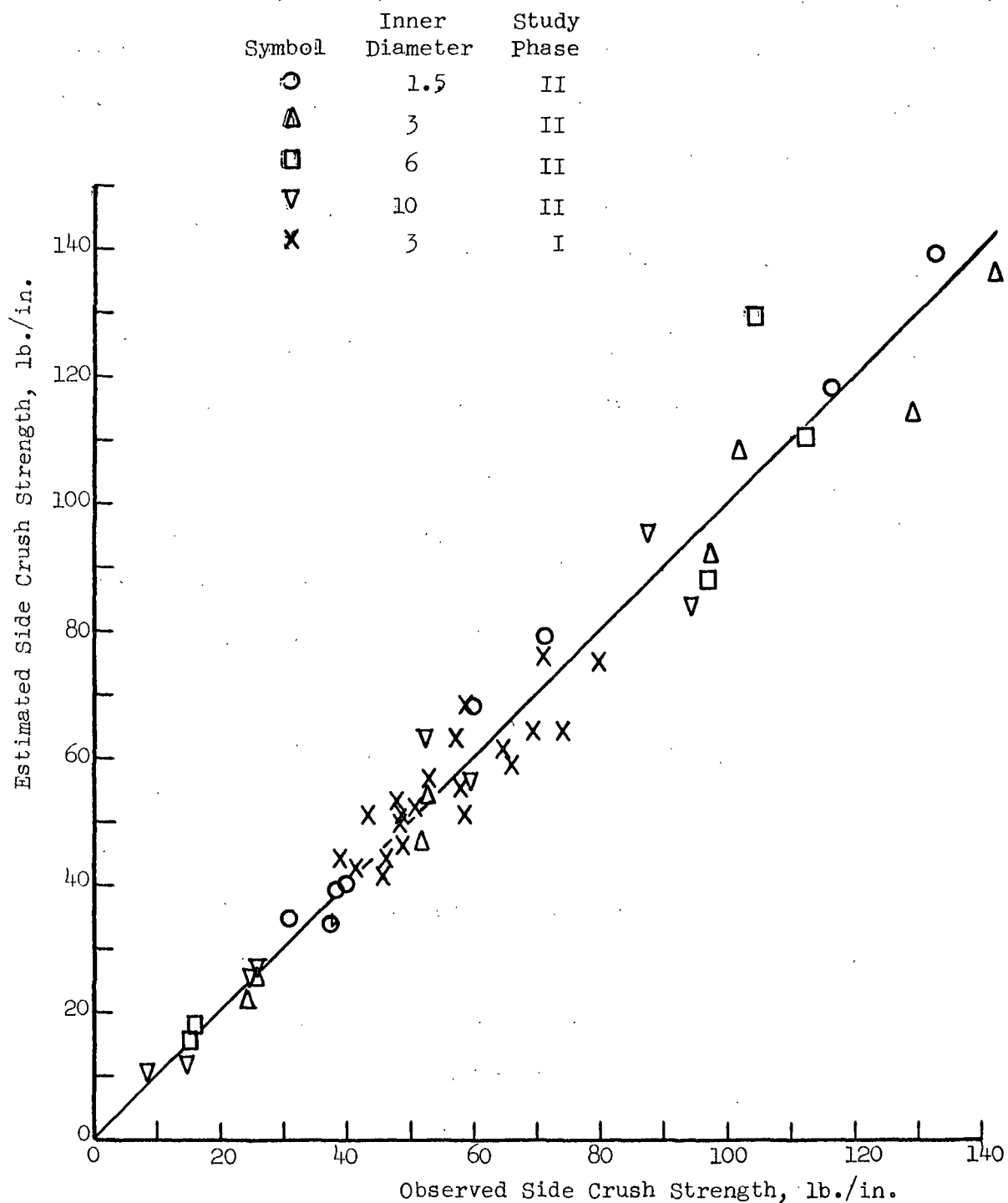


Figure 13. Final Estimates of Side Crush Strength vs. Observed Values [Equation (6)]

flattening at the loading points, and it occurs because ultimate tube failure occurs long after the onset of nonlinear behavior. Higher strength than expected may result from a very thin shape due to flattening [Ref. (1), page 124]. Furthermore, it has become apparent that ply delamination frequently occurs prior to core failure, and this further complicates the assessment of maximum core strength. Thus, it should be pointed out that the use of Equation (8) to compute nominal estimates of core side crush strength represents a compromise between different expressions, both known and unknown, which might apply more realistically to the different core geometries.

To summarize, the factors which were found to significantly influence the ultimate strength of cores when compressed from side-to-side are the following:

1. Core stock modified ring strength in a direction corresponding to the complement of the winding angle, or in the cross-machine direction. Side crush strength was found to increase when either of these core stock strength properties were increased.
2. Core winding angle. Side crush strength was found to increase with increased winding angles. But Phase II data indicated that the trend is not as great as was expected from nominal estimates. Counterbalancing effects are apparently involved with this factor.
3. Core wall thickness. Side crush strength was found to increase as the wall thickness increased, but not as much as expected from nominal estimates.

4. Core inner diameter. Strength was found to decrease as the core inner diameter was increased, but the effect was less than expected from nominal estimates.

### Beam Strength

#### Effect of Diameter and Wall Thickness

The effects of changing diameter and wall thickness on the strength of cores when loaded as a beam at three points are shown in Fig. 14 and 15 and Fig. 16 and 17 for 36 and 72-inch span beams, respectively. In Fig. 14 and 16 beam strength is plotted vs. the square of the inner core diameter. It is evident from these graphs that increasing core diameter causes an increase in beam strength, and that to a fair approximation beam strength is proportional to the square of the inner core diameter. Figures 15 and 17 illustrate the trends of the data when wall thickness is changed and inner diameter is held constant. Beam strength evidently increases as wall thickness increases and is approximately proportional to the first power of wall thickness.

These basic trends are in agreement with estimates made from a previously derived equation [Ref. (1), page 96]. That equation is the following:

$$P_{\text{nom},b} = \frac{\pi(D_o^4 - D_i^4)}{8 L D_o h_c} P_{m\alpha} \quad (10)$$

where  $P_{\text{nom},b}$  = nominal estimation of beam strength, lb.

$D_o = D_i + 2(n + 1)h_c$   
= outer core diameter, in.

$D_i$  = inner core diameter, in.

$n$  = number of core stock plies

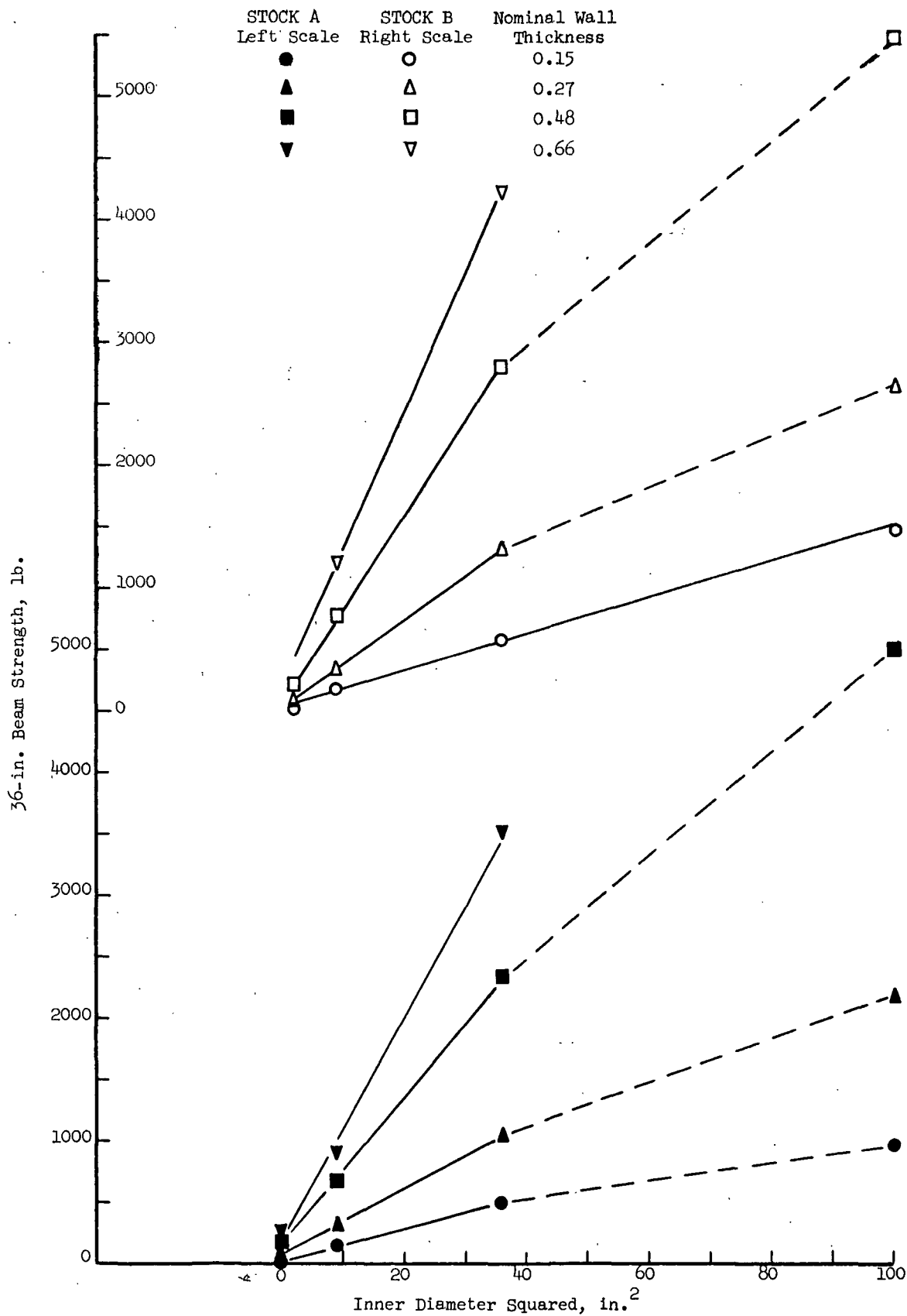


Figure 14. Observed 36-Inch Beam Strength vs. Inner Core Diameter Squared

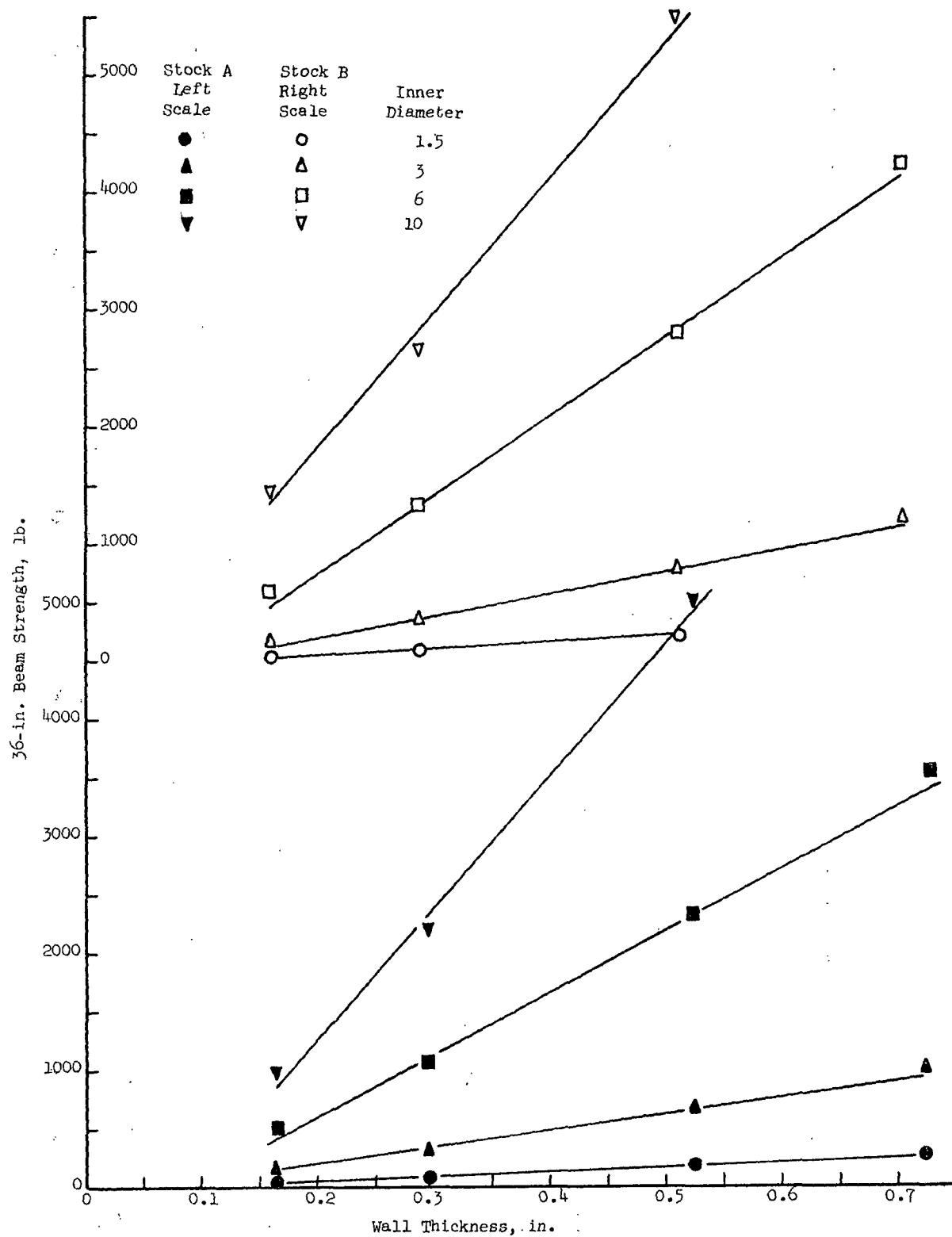


Figure 15. Observed 36-Inch Beam Strength vs. Core Wall Thickness

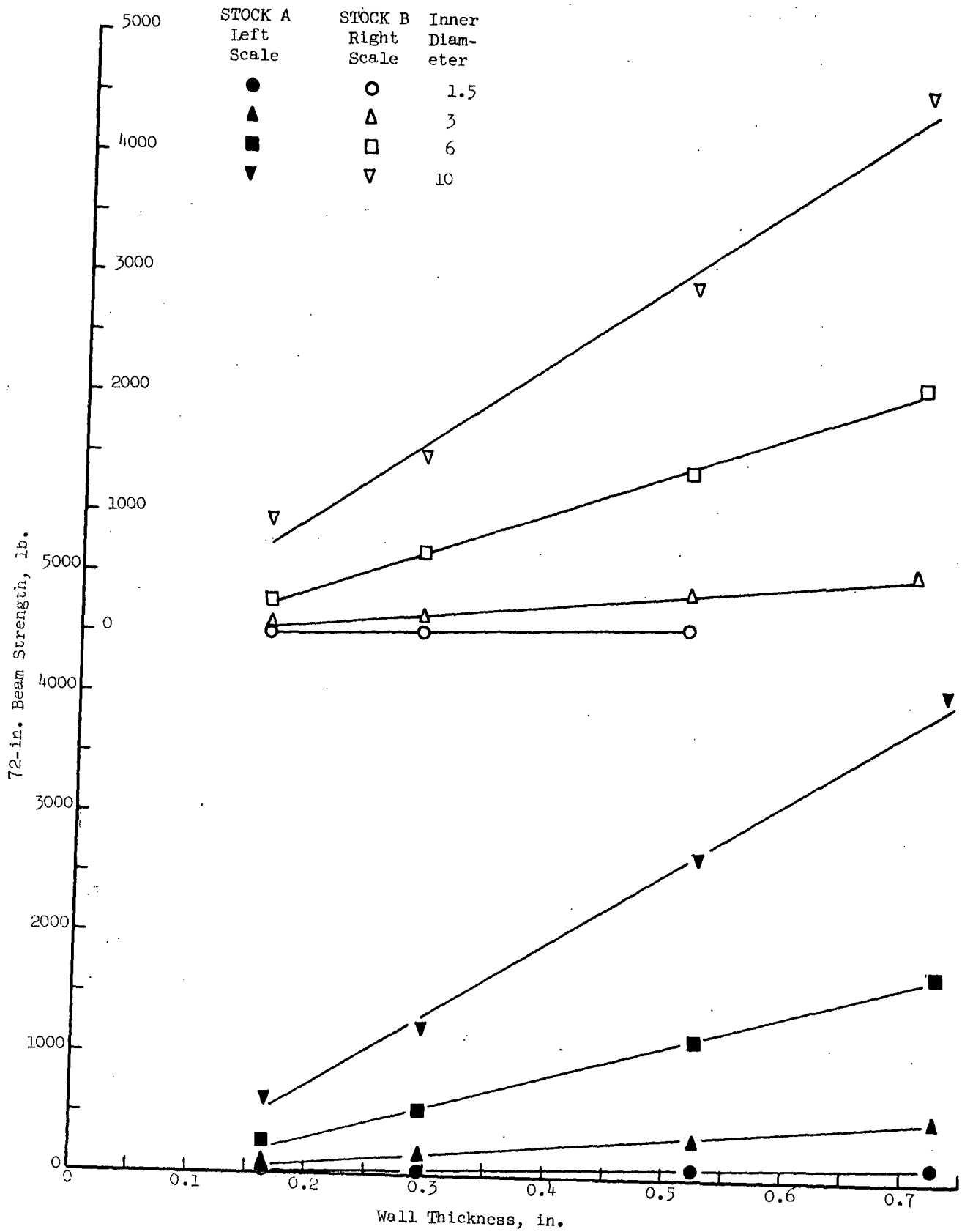


Figure 17. Observed 72-Inch Beam Strength vs. Core Wall Thickness

$\underline{h}_c$  = core stock thickness, in.

$\underline{L}$  = length of span between two simple supports, in.

$\underline{P}_{m\alpha}$  = modified ring compression strength of core stock at an angle  $\alpha$  degrees from M.D., lb./in.

$\alpha$  = angle of wind; angle between core stock M.D. and core axis, degree

Since wall thickness does not appear explicitly in Equation (10) and diameter is represented in a complex manner, it is not readily apparent from inspection that the trends illustrated in Fig. 14 through 17 are represented by Equation (10). But a rearrangement and substitution of terms into Equation (10) reveals that, to a first approximation, beam strength is theoretically proportional to the square of inner core diameter and the first power of wall thickness. Once again, however, Equation (10) by itself did not provide sufficiently accurate estimates of beam strength, and a number of adjusting factors were required. The necessity of adjustments is illustrated by Fig. 18 and 19 in which observed beam strength is plotted vs. the section modulus for 36 and 72-inch span beams, respectively. The following equation is a more general representation of Equation (10) and will explain the choice of scales in Fig. 18 and 19:

$$P_{nom,b} = \frac{4}{L} \frac{P_{m\alpha}}{h_c} \frac{I}{z} \quad (11)$$

Thus, for a given span and core stock, in which ring strength and thickness are fixed, a plot of nominal beam strength vs. section modulus,  $\underline{I/z}$ , should result in a single straight line passing through the origin. It is apparent from Fig. 18 and 19, however, that for both core stocks and spans a diameter effect exists which causes an offset between the various lines of constant diameter. Statistical analysis confirms this conclusion and also

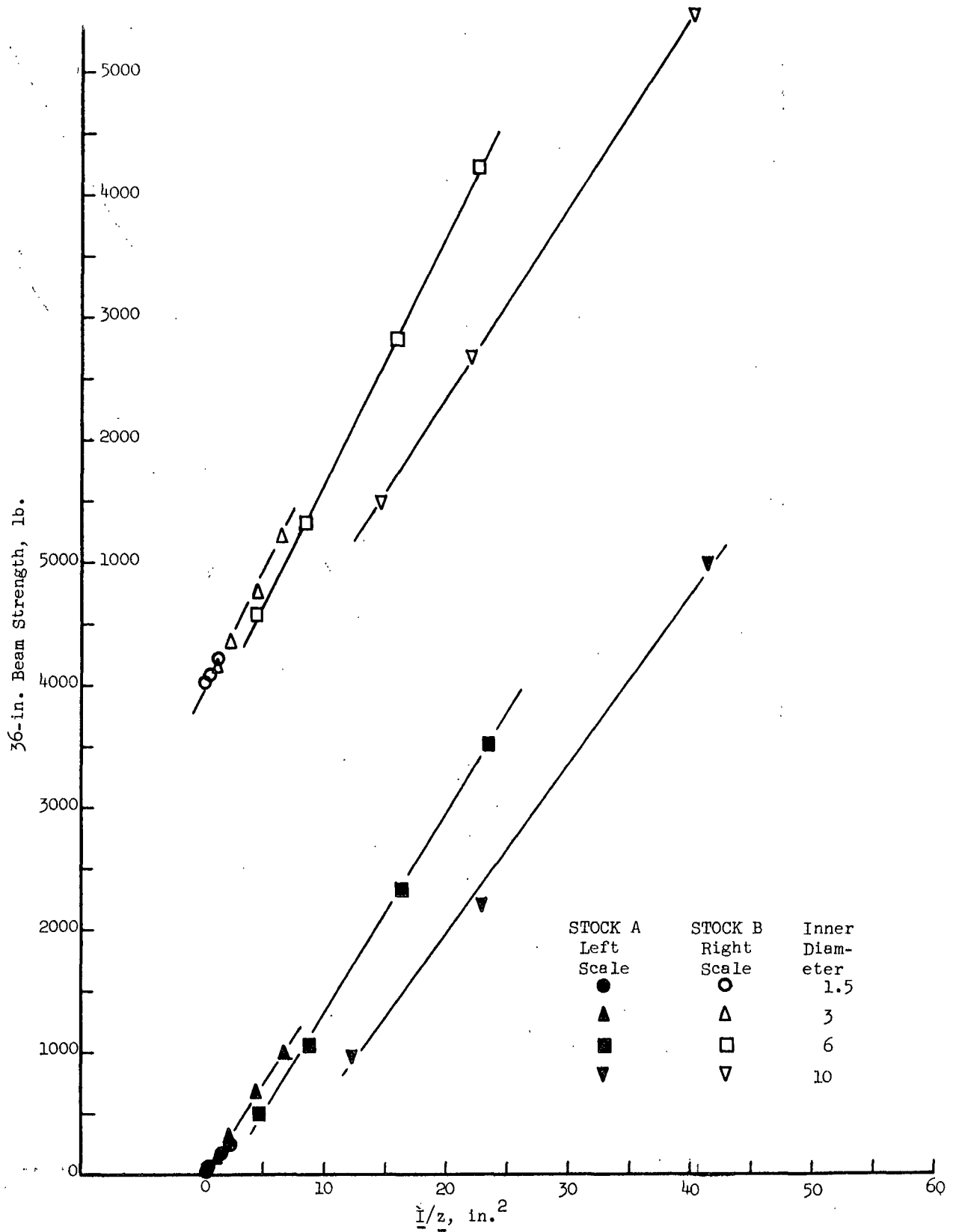


Figure 18. Nominal Estimates of 36-Inch Beam Strength vs. Section Modulus [Equation (7)]

indicates the need for additional terms involving wall thickness, winding angle, and span length.

#### Strength Equation

The final form of the strength equation to be used to estimate the beam strength of both 36 and 72-inch span beams is the following:

$$P_b = P_{\text{nom},b} \{0.45540 - (0.00717) L/D_i + (0.49133)(n + 1)h_c + (0.00184) L + (1.28887) \cos \alpha\} \quad (12)$$

where  $P_b$  = beam strength, lb.

$P_{\text{nom},b}$  = nominal estimate of beam strength, defined by Equation (10), lb.

When estimates computed from Equation (12) were compared with the test results from both Phase I and Phase II, the average prediction error was found to be 5.78% and the correlation coefficient was 0.850. Plots of estimated vs. observed beam strength values are shown in Fig. 20 and 21.

Comments similar to those made concerning other loading modes apply to the presence of the winding angle term. Once again the correction is one which causes decreases in beam strength for increases in winding angle, even though winding angle is accounted for in the nominal equation, Equation (10). The effect of the wall thickness correction term is to increase the estimate of beam strength for an increased wall thickness. A possible explanation for this effect is similar to that offered for axially loaded cores.

The  $L/D_i$  term may be interpreted as the well-known span/depth ratio correction term. The effect of this term is to modify the nominal estimate so

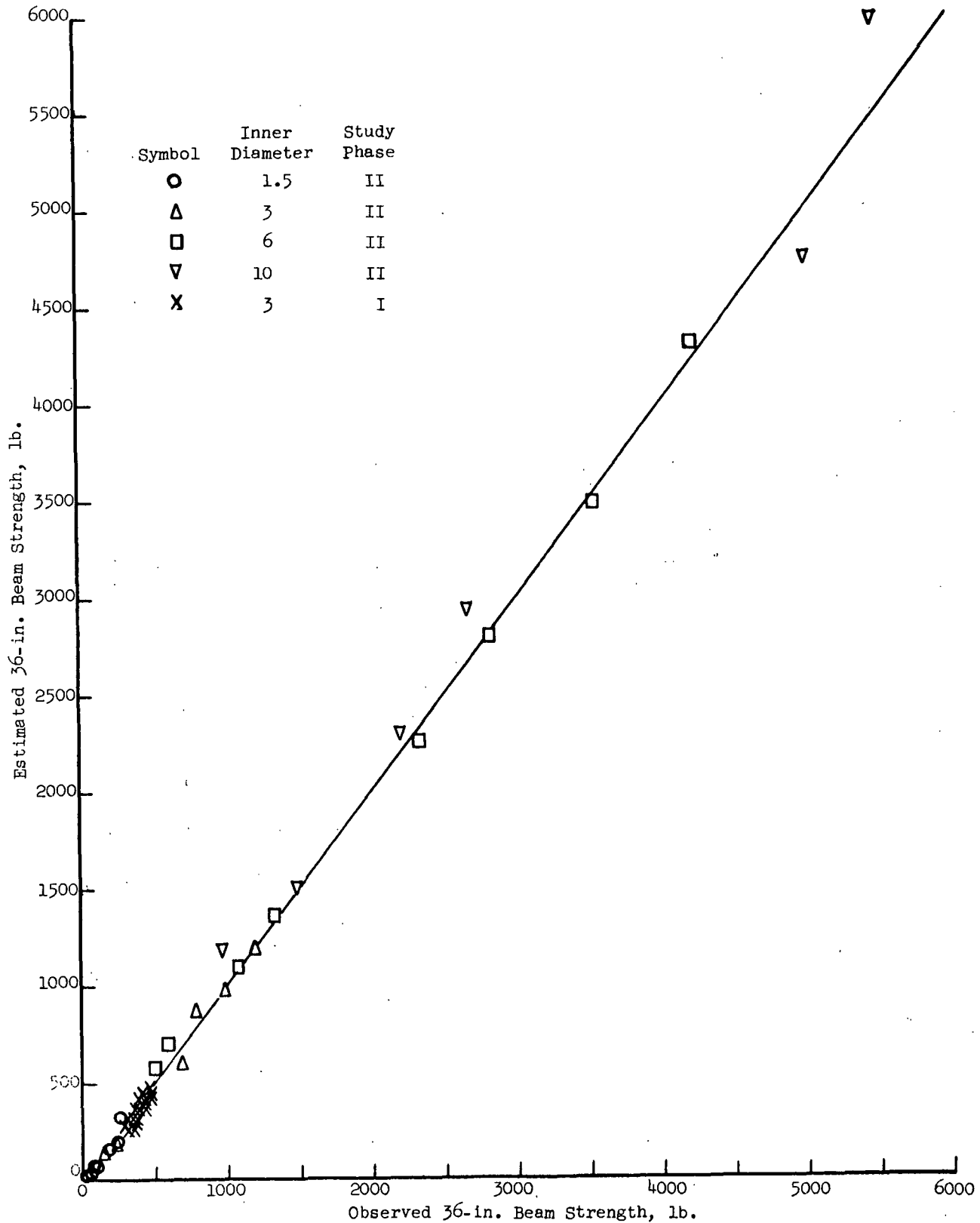


Figure 20. Final Estimates of 36-Inch Beam Strength vs. Observed Values [Equation (9)]

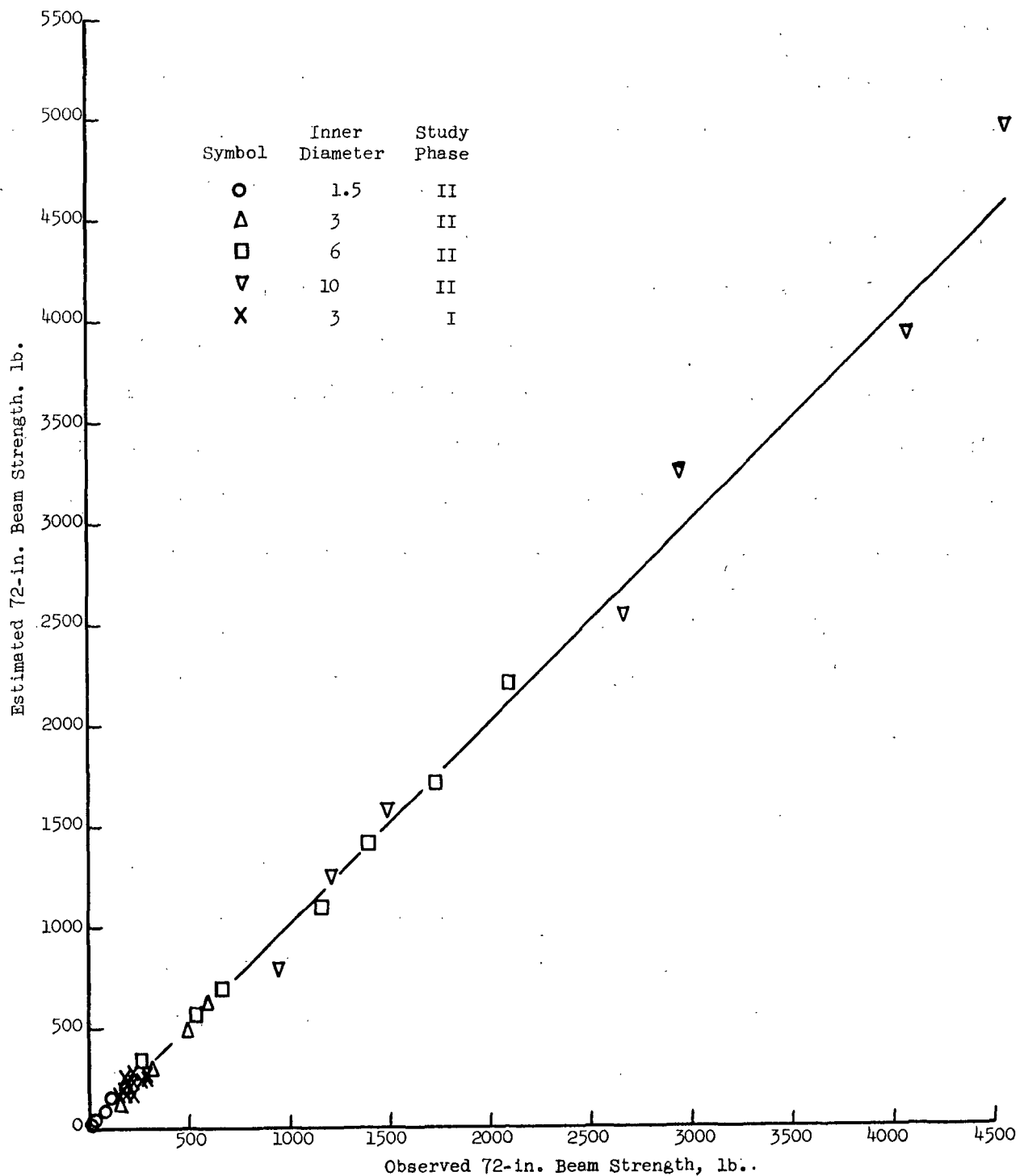


Figure 21. Final Estimates of 72-Inch Beam Strength vs. Observed Values [Equation (9)]

that, for a given diameter, the strength estimates for 72-inch span beams are somewhat less than one-half those for the 36-inch span beams.

The length correction term is believed to pertain to another phenomena which was observed during testing of the 10-inch diameter beams. These large diameter beams provided the highest section modulus to resist bending and thus could be expected to fail at relatively high loads. And yet because the cores were so thin (high  $D/T$ ), the capacity to resist radial section deformation at the loading points was very low. Consequently, severe section deformation occurred for these beams, particularly for the 36-inch span ones (Fig. 2). The problem was less severe for the longer beams since the ratio of bending stress to shear stress was twice as large for the 72-inch beams as for the 36-inch ones. Thus, the length correction term serves to reduce the estimated strength of 36-in. beams relative to 72-inch ones when the diameter/wall thickness ratio is so large that severe radial deformation occurs at the loading points.

In summary, the factors which were found to significantly influence the ultimate strength of cores when loaded as a three-point beam are the following:

1. Core inner diameter. Beam strength was found to increase as inner diameter was increased, it being approximately proportional to the square of the inner diameter.
2. Core stock modified ring strength in a direction corresponding to the winding angle, or in the cross-machine direction. Strength was found to increase as either of these core stock properties was increased.

3. Core winding angle. Beam strength was found to decrease as the winding angle was increased. Data from Phase II indicated that the strength decrease was larger than was expected from nominal estimates.
4. Core wall thickness. Beam strength was found to increase as wall thickness was increased, and to a greater extent than was expected from nominal estimates.
5. Span. Beam strength was found to decrease as the span was increased, being roughly inversely proportional to the span. In addition, a small span/diameter term was found to be significant, causing longer span beams to be slightly weaker than expected from nominal estimates. For beams of large diameters (10 inch) and thin walls (0.48 inch or less) resistance to radial deformation was found to be so small that premature failure was noted for the shorter 36-inch beams.